Variability of ice supersaturated regions at flight altitudes: evaluation of ERA5 reanalysis using IAGOS in situ measurements

Katarina Grubbe Hildebrandt[1], Federica Castino[1], Vincent Meijer[1], and Feijia Yin[1]

[1]Delft University of Technology, Faculty of Aerospace Engineering, Delft, The Netherlands

Correspondence: Katarina Grubbe Hildebrandt (k.g.hildebrandt@tudelft.nl) and Feijia Yin (f.yin@tudelft.nl)

Abstract. Contrail cirrus is ~~one of the largest contributors~~ a major contributor to aviation's radiative forcing, ~~which arises~~ arising from long-lived persistent contrails. Avoiding persistent contrail formation has been suggested as a measure to reduce the climate impact of aviation, requiring accurate forecasts of ice supersaturated conditions, i.e. where the relative humidity over ice (RHi) exceeds 100%. Numerical weather prediction ~~(NWP) models~~ models and reanalysis products often underestimate or do not account for ice supersaturation. This study evaluates ice supersaturated regions (ISSRs) in the ECMWF ERA5 reanalysis dataset using In-service Aircraft for a Global Observing System (IAGOS) measurements over tropical and extratropical regions in the upper troposphere and lower stratosphere ~~for the period 2011–2022. It considers~~ from 2011 to 2022. It considers seasonal and vertical differences, and the effect of cloudy and clear-sky conditions ~~and how North Atlantic weather patterns affect the ERA5 ability~~ on the ability of ERA5 to predict ISSRs. ERA5 generally underestimates ISSR occurrence due to a dry bias in RHi; the equitable threat score (ETS) is 0.2~~–0.4~~–0.4, indicating a weak to mediocre relationship with IAGOS. Lowering the ERA5 RHi threshold improves ISSR prediction, with the largest improvements found for RHi values between 85% and 95%, although the optimal threshold varies with distance to the tropopause, region and season. Clear-sky conditions result in an ETS of 0.05~~–0.18 and generally~~ –0.18, while the ETS is mostly below 0.1 in cloudy conditions, indicating an almost random relationship. ~~The latter is the result of the saturation adjustment used by the NWP model underlying the reanalysis. North Atlantic winter weather patterns appear to affect the ability of~~ Lowering the ERA5 ~~to predict ISSRs, particularly along eastbound routes. This may result from varying ISSR distributions relative to the jet stream. North Atlantic summer weather patterns show little impact due to weaker teleconnection patterns. Overall, the underestimation of ISSRs~~ RHi threshold to 75%–85% increases the ETS by approximately 0.1 in ~~ERA5 is most critical in the upper troposphere, where their occurrence is highest~~clear-sky conditions. In cloudy conditions, lowering the threshold shows little benefit because increases in correctly predicted ISSRs are offset by increases in false positives.

1 Introduction

The aviation industry is ~~an important~~ a significant contributor to anthropogenic climate change. In 2018, aviation accounted for 2.5% of the world's CO_2 emissions ~~(Lee et al., 2021; Teoh et al., 2022; Wolf et al., 2023)~~(Lee et al., 2021). Aviation has also been estimated to contribute to 3.5% to 5% of global anthropogenic radiative forcing (Lee et al., 2021). The anthropogenic radiative forcing is due to CO_2 and non-CO_2 emissions, which include NO_x emissions, H_2O, soot, contrails, and

contrail cirrus (Lee et al., 2009). The best estimate of contrail cirrus effective radiative forcing is almost twice as large as that of CO_2, but is also subject to ~~much larger uncertainties~~ a much larger uncertainty range than that of CO_2 (Lee et al., 2021). This is due to a ~~large number of sources of uncertainty~~ number of uncertainty sources in the evaluation of contrail cirrus~~(Wilhelm et al., 2021)~~, related to the radiative transfer calculations, the upper tropospheric water budget and the modelling of contrail cirrus (Lee et al., 2021).

One solution to lowering the climate impact of aviation is to minimise the radiative forcing due to contrail cirrus. Contrail cirrus is the result of the dispersion of persistent contrails. Contrails form when the Schmidt-Appleman criterion (SAC) is met ~~(Schumann, 1996; Gierens et al., 2020a)~~(Schumann, 1996), and persist when the ambient air is supersaturated with respect to ice, i.e. relative humidity over ice (RHi) is greater than 100% (Gierens et al., 2020a; Wolf et al., 2025). A region where the latter occurs is called an ice supersaturated region (ISSR) (Reutter et al., 2020). Reducing persistent contrails can be realised by avoiding flying through ISSRs (Mannstein et al., 2005; Filippone, 2015; Yin et al., 2018; Avila et al., 2019; Teoh et al., 2020; Martin Frias et al., 2024; Sausen et al., 2024; Sonabend-W et al., 2024). This requires accurate predictions and evaluations of ice supersaturation (ISS). However, ISS is often not accounted for or underestimated in numerical weather prediction (NWP) models ~~(Rädel and Shine, 2010; Gierens et al., 2020a; Wilhelm et al., 2022; Agarwal et al., 2022; Wolf et al., 2023)~~and reanalysis products (Rädel and Shine, 2010; Gierens et al., 2020a; Wilhelm et al., 2022; Agarwal et al., 2022; Wolf et al., 2023; Thompson et al., 202
.

The lack of ISS in NWP models ~~has been shown to arise due to several reasons~~and reanalysis products has been attributed to several factors. One reason is the large temporal and spatial variability of the humidity field, ~~with~~ which exhibits sharp gradients (Wilhelm et al., 2022; Sperber and Gierens, 2023; Wolf et al., 2025). ~~It is also due to a lack~~ Another factor is the limited availability of reliable relative humidity measurements at aircraft cruise altitudes (Sperber and Gierens, 2023) and due to the coarse resolution of weather models (Gierens et al., 2012). This leads to biases in the prediction of relative humidity in weather models. Reutter et al. (2020) showed that ERA-Interim, the predecessor of ERA5, underestimated RHi when greater than 100%, leading to an underestimation in the occurrence of ISS when compared to MOZAIC (Measurement of OZONE and Water Vapour on Airbus in-service Aircraft), which is currently part of IAGOS. It has also been shown that ERA5 has a dry bias when RHi is above 100%, when compared to MOZAIC/IAGOS (In-Service Aircraft for Global Observing system) ~~(Gierens et al., 2020a; Schumann et al., 2021; Teoh et al., 2022; Wolf et al., 2025). Contrarily,~~ (Gierens et al., 2020a; Schumann et al., 2021; Teoh et al., 2022; Thompson et al., 2024; Wolf et al., 2025). Dyroff et al. (2014), Shepherd et al. (2018) and Bland et al. (2021) have shown a moist bias in the lower stratosphere of the ECMWF Integrated Forecasting System (IFS). Meanwhile, there are often good agreements in temperature between model predictions and measurements (Dyroff et al., 2014; Reutter et al., 2020; Wolf et al., 2025). Beyond these biases, recent work suggests that ISS representation in models may also be affected by synoptic conditions. Driver et al. (2025) found that ERA5 poorly captures ISS conditions in the dry intrusions over the North Atlantic.

Another ~~reason for~~ important factor contributing to the underestimation of RHi in NWP models and reanalysis products is related to the representation of the physics of the cloud nucleation process (Dyroff et al., 2014). Previously, supersaturation with respect to ice was not allowed in models such as the ECMWF IFS (Dyroff et al., 2014). However, the ECMWF IFS now

uses ~~the~~ a saturation adjustment in the ice cloud microphysical scheme ~~to allow~~ that allows for ISS (Tompkins et al., 2007; Wolf et al., 2025). ~~The saturation adjustment can be explained as when~~ When cloud formation occurs in an ice supersaturated grid box with this saturation adjustment, RHi is lowered to 100% within the cloudy part of the grid-box in the next time step (Tompkins et al., 2007; Straka, 2009; Sperber and Gierens, 2023). Recent work has focused on improving cloud cover and ice microphysical parametrizations. For example, Hanst et al. (2025) demonstrated that the ICON NWP model captures ice supersaturation more accurately when using a two-moment ice microphysics scheme compared to a one-moment scheme that limits ISS representation. Similarly, a modified cloud scheme in the ARPEGE NWP model showed improved representation of ice supersaturation, although it remains limited in the maximum RHi values that can be attained (Arriolabengoa et al., 2025).

In clear-sky conditions, models such as the IFS ~~,~~ can also represent ISS (Tompkins et al., 2007; Reutter et al., 2020). However, ERA5, generated with the ECMWF IFS Cycle 41r2, shows a lack of ISS under (almost) clear-sky conditions in the mid-latitudes, as reported by Wolf et al. (2025). Wang et al. (2025) ~~also~~ showed that ERA5 was limited in predicting ISSRs under clear-sky conditions. Hence, issues in the representation of ISS occurs in both cloudy and clear-sky conditions in ERA5.

Many of the studies analysing the accuracy of NWP models ~~in~~ and reanalysis products in the prediction of ISS compared to observations, ~~i.e.~~ e.g. MOZAIC/IAGOS, are often limited in terms of regional and seasonal variations. The main area of interest are the mid-latitude regions as this is one of the most sampled regions by MOZAIC / IAGOS aircrafts (Reutter et al., 2020; Sanogo et al., 2024; Wolf et al., 2025). Only Gierens et al. (2020a) compared IAGOS and ERA5 below a latitude of 30° N, considering four months in 2014. The entire MOZAIC/IAGOS framework now spans more than 20 years (Reutter et al., 2020). Furthermore, there are limited comparisons of RHi and ISS between the subregions of the globe. In some instances, this is due to a smaller focused area, i.e. the North Atlantic corridor. Reutter et al. (2020) selected a larger region, considering North America, the North Atlantic corridor, and Europe, but the analysis on regional variations were limited. In case of the study by Gierens et al. (2020a), variations due to different climates (tropics versus extratropics) is not included. Thus, there is a need to further quantify regional ~~, including climate,~~ dependence of the differences in ISS between the weather model predictions and observations, in particular, the IAGOS measurements.

Additionally, previous research shows that the occurrence of ISSRs has a seasonal dependence. Globally, this has been shown by Gierens et al. (1999) and Spichtinger et al. (2003b), and in the northern mid-latitudes ~~(Petzold et al., 2020) and over~~ by Petzold et al. (2020). Regional studies include the Paris area (Wolf et al., 2023) ~~. Gierens et al. (2012) also showed a seasonal variation in ISSR occurrence, with less ISSRs from April to September over the Lindenberg meteorological observatory. Petzold et al. (2020) showed varying ISSR and RHi seasonality~~ and the Meteorological Observatory Lindenberg (Spichtinger et al., 2003a; . Seasonality also varies regionally, as demonstrated by Petzold et al. (2020) between Europe, the North Atlantic ~~Corridor~~ corridor and eastern North America. However, ~~the~~ seasonal differences in ISSR occurrence between observations and NWP models as well as reanalysis products are rarely considered. Gierens et al. (2020a) analysed seasonal differences in RHi and ISS between IAGOS observations and the ERA5 reanalysis considering four months ~~of one year of data~~in 2014, with each month representing a season; some seasonal dependency on the differences between IAGOS and ERA5 was identified. Since the study only considered a four month dataset, it has a high potential to be expanded with extensive input data. Also, no

analysis of seasonal differences as a function of geographic region appears to have been performed. Hence, it is important to further quantify these differences between observations and weather models.

~~A region of particular interest is the North Atlantic corridor, one of the busiest air traffic corridors (Teoh et al., 2022). Irvine et al. (2012) found that the probability of forming contrails as a function of altitude depends on the weather patterns when using ERA-Interim. This raises the question of whether the type of weather pattern can affect the observed biases in ERA5 as well.~~

Therefore, the aim of this study is to further investigate differences in ISS between the ECMWF ERA5 reanalysis and IAGOS in situ measurements, with an ~~expanded geographical~~ extensive geographical and temporal area. Differences will be analysed from a regional and seasonal perspective, to understand if certain conditions might lead to a drier or more moist bias in ERA5. The impact of clouds on differences in ISS between IAGOS and ERA5 will also be analysed on ~~a larger~~ an extended geographical scale. ~~Lastly, it will be investigated if different winter and summer weather patterns in the North Atlantic corridor impact the ability of~~ We also investigate if changing the ERA5 ~~to predict ISSRs~~ RHi threshold allows for better prediction of ISSRs in ERA5.

Section 2 describes the datasets and the methodology used in this study. Section 3 documents differences in temperature and RHi and the impact of the prediction of ISSRs. ~~This section also documents the influence of different weather conditions on the ability of ERA5 to predict ISS~~In Sect. 4, we discuss the findings and compare to previous literature. Lastly, conclusions are drawn in Sect. 5.

2 Data and methodology

~~This section explains the data selection from the IAGOS in situ measurements and the method to evaluate the ERA5 reanalysis.~~

2.1 IAGOS

IAGOS (Petzold et al., 2015) provides atmospheric composition measurements from commercial aircraft and was founded in 2011 (IAGOS, last access: 2025-04-15a). It is the successor of the MOZAIC programme and the Civil Aircraft for the Regular Investigation of the Atmosphere Based on an Instrument Container (CARIBIC), which began measurements in 1994. Meanwhile, MOZAIC is no longer a project, CARIBIC continues within IAGOS and serves as a reference standard for the rest of the IAGOS fleet (Petzold et al., 2015).

The IAGOS-CORE component is installed on long-range aircraft from internationally operated airlines (Petzold et al., 2015), ~~where~~ with 10 aircraft ~~are~~ currently active (IAGOS, last access: 2025-04-15d). IAGOS-CORE contains several autonomous instruments for daily measurements of reactive, ~~i.e.~~ e.g. O_3, and greenhouse gases, such as CO_2 and water vapour, as well as aerosol and cloud particles (Petzold et al., 2015). The main package installed in the entire IAGOS fleet is Package 1, which includes a humidity sensor (ICH) and a backscatter cloud probe (BCP) that measures cloud particles (IAGOS, last access: 2025-04-15c).

The ICH consists of a modified Vaisala HUMICAP® of type H sensor (capacitive relative humidity sensor) (Neis et al., 2015) and a platinum resistance sensor for temperature measurements at the surface of the humidity sensing element (IAGOS, last access: 2025-04-15b). It has the capability to provide temperature and relative humidity (with respect to liquid) measurements. The relative humidity has a precision of ± 1%, an accuracy of ± 6% and a time resolution of 1 s at 300 K to 120 s at 200 K (IAGOS, last access: 2025-04-15b). Temperature measurements have a precision of ± 0.2 K, an accuracy of ± 0.5 K and a time resolution of 4 s (IAGOS, last access: 2025-04-15b).

Given the start date of the IAGOS program and that the entire IAGOS fleet was equipped with the modified Vaisala HUMICAP® of type H sensor in 2011 (Neis et al., 2015), data measured between 1 July 2011 and 31 December 2022 have been collected for the current study. The end date is set to 31 December 2022 due to a lack of published flight measurements with all observed variables after this date (at the time of data collection). The altitude is restricted between 8000 m and 13000 m as these are the flight levels that are the most visited by IAGOS aircraft. These are also the levels where we can expect ISSRs to occur in the midlatitudes (Lamquin et al., 2012; Sanogo et al., 2024). In the tropics, ISSRs are rare below 10000 m, and have been show to occur at altitudes of more than 15000 m (Lamquin et al., 2012). Commercial aircraft do not cruise at such high altitudes, as also seen from the IAGOS dataset. Hence, we maintain the upper bound of 13000 m.

Based on the global distribution of the IAGOS measurements during the considered time frame, as seen in Fig. 1, only measurements located between 160° W and 150° E, and between ~~30~~0°~~S~~ N and 75° N will be considered. This is further divided into eight regions. The latitudes of the regions are based on the definition of ~~tropical (~~extratropical (latitude < 30°~~S ≤ latitude ≤~~ S and latitude > 30° N) and ~~extratropical regions (latitude <~~ tropical (30°~~S and latitude >~~ S < latitude < 30°~~N) (Spichtinger and Leschner, 2016). The eight~~ N) regions (Spichtinger and Leschner, 2016). We recommend considering the Northern and Southern Hemisphere tropics separately due to the inter-tropical convergence zone, which causes changes in wet and dry conditions across the equator depending on its position (National Oceanic and Atmospheric Administration, 2023), as discussed in Appendix A. Due to low sampling in the Southern Hemisphere tropics, we subsequently only focus on the Northern Hemisphere. The eight defined regions are shown in Fig. 1 and have the areal boundaries given in Table 1.

Only points with a relative humidity with respect to liquid (RHL) between 0% and 100% are selected from IAGOS measurements. A RHL greater than 100% implies flying through a liquid cloud, and contrails cannot form at temperatures where these clouds are present (Wilhelm, 2022).

IAGOS uses validity flags to indicate the quality of the measurements. The following validity flags are used: 'good' (0), 'limited' (2), 'erroneous'(3), 'not validated' (4) and 'missing value' (7) (IAGOS, last access: 2025-06-10). Only 'good' and 'limited' measurements are considered for temperature, relative humidity with respect to ice (RHi) and RHL. However, we use the RHL validity ~~to select RHI~~ flag to select RHi values since the quality flag of RHi is not well derived, but is known to be similar to that of RHL (Sanogo et al., 2024). A summary of the criteria for the IAGOS measurements is provided in Table 2.

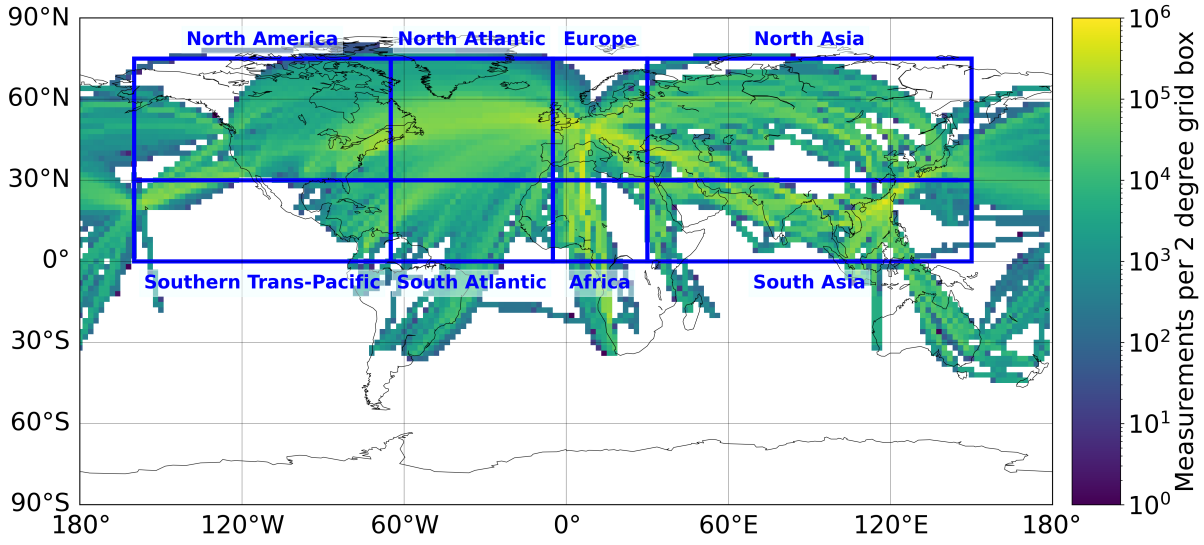

Figure 1. IAGOS measurement density map per 2°grid box with regional division between 8000 m and 13000 m from 1 July 2011 to 31 December 2022, considering 'good' or 'limited' validity flags for RHL and temperature.

Table 1. Areal boundaries of defined geographical regions.

Region	Longitude	Latitude
North America	160° W to 65° W	30° N to 75° N
North Atlantic	65° W to 5° W	30° N to 75° N
Europe	5° W to 30° E	30° N to 75° N
North Asia	30° E to 150° E	30° N to 75° N
Southern Trans-Pacific	160° W to 65° W	~~30~~0° ~~S~~ N to 30° N
South Atlantic	65° W to 5° W	~~30~~0° ~~S~~ N to 30° N
Africa	5° W to 30° E	~~30~~0° ~~S~~ N to 30° N
South Asia	30° E to 150° E	~~30~~0° ~~S~~ N to 30° N

Lastly, IAGOS records the measurements every four seconds. To avoid autocorrelation affecting our analysis, it is chosen to sample a measurement approximately every minute~~, which corresponds to 2.5% of all IAGOS measurements between 01/07/2011 and 31/12/2022. To avoid systematic bias, the data points are randomly sampled~~ . This is done using a uniform random number generator ranging from 1 to the maximum number of measurement points from IAGOS~~.~~, to avoid systematic bias. The sampling and application of the criterion from Table 2 results in using 3.8% of all IAGOS measurements between 1 July 2011 and 31 December 2022.

Table 2. Criteria for selection of IAGOS measurements.

Criterion	
Measurement dates	Between ~~01/07/~~1 July 2011 and 31 ~~/12/~~December 2022.
Altitude	Between 8000 m and 13000 m.
RHL	Between 0% and 100%.
Validity flags for ~~RHi,~~ RHL and temperature	Equal to 0 or 2, corresponding to 'good' or 'limited'.
Geographic coverage of measurements	Located between 160° W and 150° E, and between ~~30~~0° ~~S~~ N and 75° N

2.2 ERA5 reanalysis

The ERA5 reanalysis is the fifth generation reanalysis from ECMWF (Hersbach et al., 2020). To allow for a higher vertical resolution, the Analysis-Ready, Cloud Optimized (ARCO) ERA5 (Carver and Merose, 2023) has been used, which provides several atmospheric variables on model levels. ARCO ERA5 was retrieved using the python library pycontrails (Shapiro et al., 2025), which also allows for the re-gridding of model levels to pressure levels. It was chosen to re-grid with a vertical resolution of 10 hPa. This is within the range of the model level resolution at typical cruise altitudes, which is between 8 hPa and 15 hPa when considering a surface pressure of 1013.250 hPa (ECMWF, last access: 2025-05-07).

The ERA5 reanalysis is (quadrilinearly) interpolated in time, pressure level, longitude and latitude onto the IAGOS flight tracks using the Delftblue supercomputer (Delft High Performance Computing Centre, 2024). ~~The~~ Since the ARCO ERA5 dataset does not provide RHi~~and RHL, hence~~ , it is derived from specific humidity, temperature and the saturation water vapour pressure over ~~liquid water and~~ ice are used to calculate ~~these two variables.~~ RHi. The saturation water vapour pressure over ice is computed using the AERKI formula of Alduchov and Eskridge (1996) to be consistent with the ECMWF IFS formulation (European Centre for Medium-Range Weather Forecasts (ECMWF), 2016). RHi is calculated only for temperatures below 250.15 K (Hersbach et al., 2023a). However, specific humidity exhibits a nonlinear lapse rate (pycontrails, 2025). ~~Thus, to~~ To avoid biases due to linear interpolation, ~~RHL and RHi should be~~ RHi is therefore calculated before interpolation, where we then interpolate in the RHi ~~and RHL~~ space (pycontrails, 2025).

2.3 Vertical distribution of variables with respect to tropopause

The vertical distribution of the temperature, relative humidity over ice, and ISSR fraction will be reported relative to the tropopause height. Both the dynamic and thermal tropopause have been considered, and were determined using ERA5 tropospheric data reported by Hoffmann and Spang (2022). Given the stronger gradients in temperature and RHi associated with the thermal tropopause (see Appendix B), the results are presented relative to this definition. This will, for example, result in a drier lower stratosphere compared to ~~if~~ using the dynamic tropopause definition~~was used~~.

The flight measurements are distributed into layers with a thickness of 30 hPa, centered at the tropopause. The selection of layers for further analysis depends on the number of data points per level, which varies per geographical region, as seen in

Fig. 2. This figure shows that in the extratropic regions, the majority of measurements are distributed around the tropopause, allowing for upper tropospheric and lower stratospheric analysis. In the tropics, most of the samples are located in the upper troposphere since the tropopause is located at higher altitudes in this region.

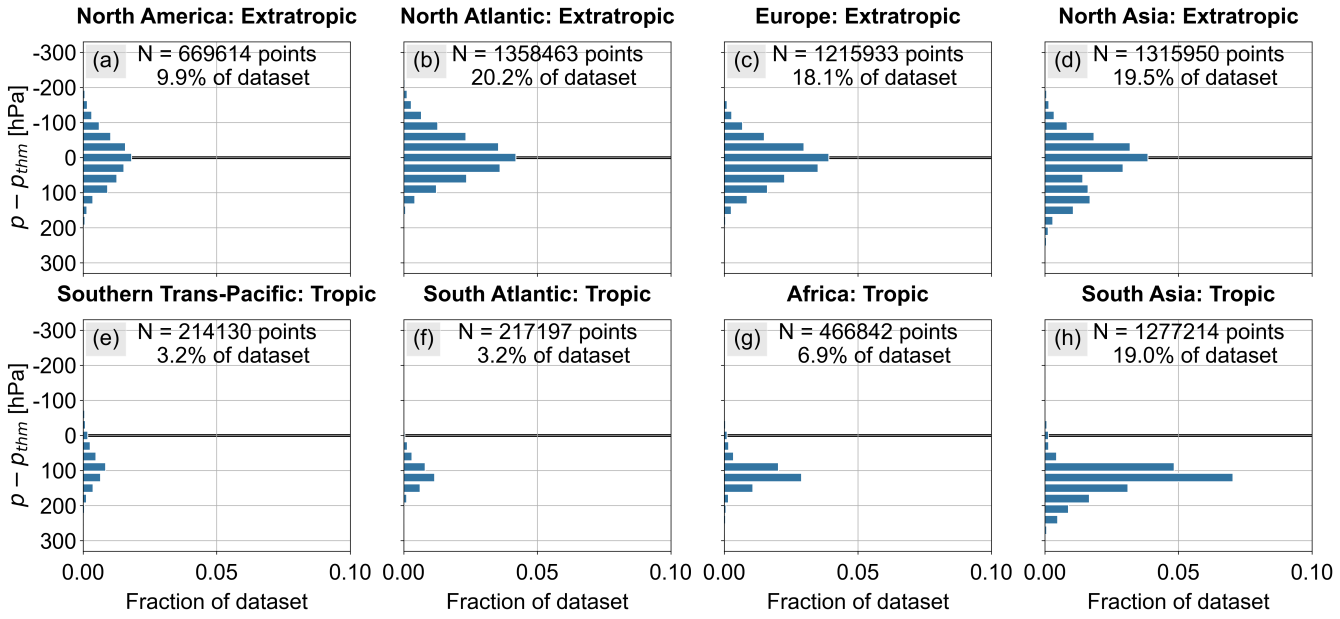

Figure 2. ~~(a-h)~~(a–h)Vertical distribution of number of samples with respect to distance to the thermal tropopause, ~~p_{thm}~~$p - p_{thm}$, in different geographical regions.

2.4 Differentiation of cloudy and clear-sky conditions

To investigate the impact of cloudy and clear-sky conditions on the ability of ERA5 to predict ISS, we need to distinguish between these two conditions. For IAGOS, the ~~number of ice particles~~ice crystal number concentration, N_i, can be used to differentiate between measurements within cirrus clouds and within cloud-free conditions. We use the same thresholds defined by Petzold et al. (2017), which ~~can be summarised as follows:~~

~~Cloudy: $N_i \geq 0.015$ cm^{-3} Clear-sky: $N_i \leq 0.001$ cm^{-3} Indeterminate: $0.001 < N_i < 0.015$ cm^{-3}. This refers~~ are summarised in Table 3. Indeterminate conditions refer to measurements that cannot be identified as clouds and cannot be considered cloud-free. These measurements are most likely located within very thin cirrus (Petzold et al., 2017) ~~.~~

~~The fraction of cloudy, clear-sky and indeterminate conditions, based on the definition of the number of ice particles, per layer and geographical region is visualised in Fig. 3. The majority of samples are categorised as no clouds or no measurements. There are few indeterminate and cloudy conditions. The low number of cloud observations is in line with reports from Sanogo et al. (2024).~~

For the ERA5 reanalysis, cloudy and clear-sky conditions can be differentiated using the cloud cover fraction, CC, which takes a value between 0 and 1. CC describes the proportion of a grid box covered by liquid or ice clouds (Hersbach et al., 2023a). For the analysis of RHi and ISSRs, we only consider data points where the temperature is below 235.15 K, which is below the threshold at which liquid clouds can occur (Gierens et al., 2020b), hence we focus on ice clouds. To distinguish between cloudy, clear-sky and indeterminate conditions, we use the same thresholds as Wolf et al. (2025)~~:~~, which are also defined in Table 3.

~~Cloudy:~~

Table 3. Thresholds used to define cloudy, clear-sky and indeterminate conditions in IAGOS and ERA5.

	IAGOS	ERA5
Cloudy	$N_i \geq 0.015$ cm^{-3}	$0.8 \leq CC \leq 1$ ~~Clear-sky:~~
Clear-sky	$N_i \leq 0.001$ cm^{-3}	$CC < 0.2$ ~~Indeterminate:~~
Indeterminate	$0.001 < N_i < 0.015$ cm^{-3}	$0.2 \leq CC < 0.8$

The fraction of cloudy, clear-sky and indeterminate conditions, based on the definition of the ice crystal number concentration in IAGOS, per layer and geographical region, is visualised in Fig. 3. The majority of samples are categorised as no clouds or no measurements. There are few indeterminate and cloudy conditions. The low number of cloud observations is in line with reports from Sanogo et al. (2024).

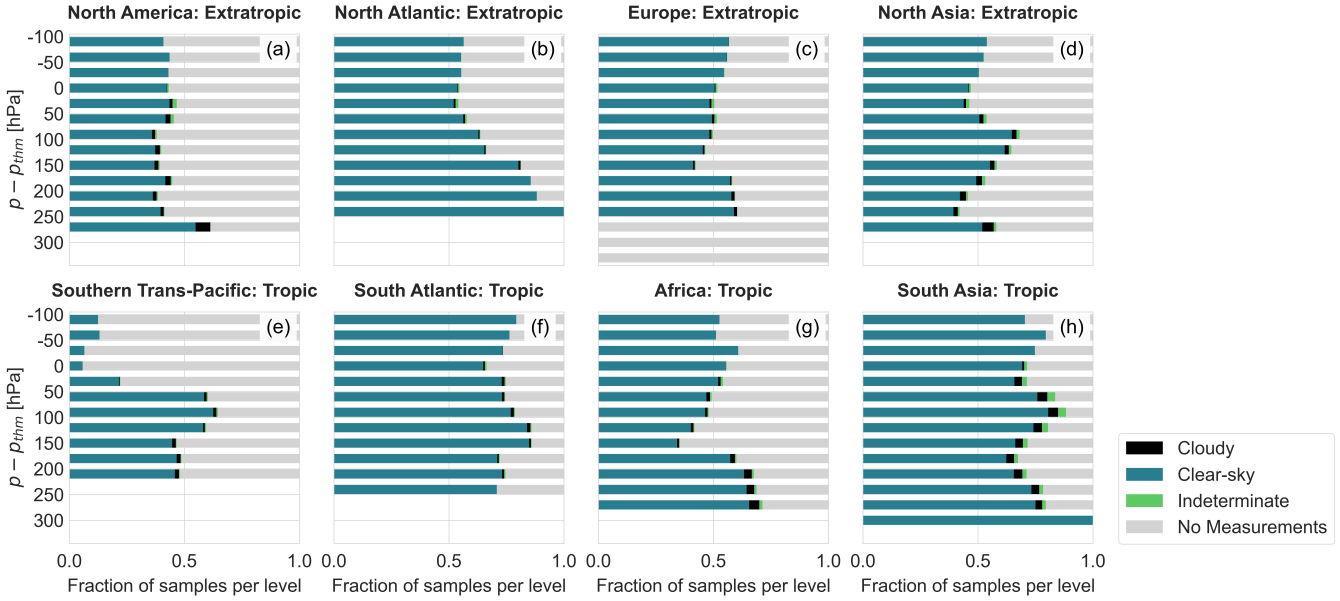

Figure 3. ~~(a–h)~~(a–h) Fraction of cloudy, clear-sky and indeterminate conditions per layer and geographic region, based on the ice crystal number concentration, N_i, from IAGOS measurements. No measurements means that there is no data available on the ice crystal number concentration from IAGOS.

The application of cloud cover to determine cloudy, clear-sky and indeterminate conditions using ERA5 results in the division seen in Fig. 4. We applied the 'no measurements' label to ERA5 for the same points as in IAGOS.

Comparing Fig. 3 and Fig. 4, it is noticeable that there are discrepancies in the labelling of cloudy, clear-sky and indeterminate conditions between IAGOS and ERA5. We see that ERA5 shows a higher frequency of indeterminate and cloudy conditions compared to IAGOS. However, the choice of definition to use to define cloudy and clear-sky conditions in IAGOS and ERA5 largely impacts the results as shown by the sensitivity study presented in Sect. S1 of the supplement.

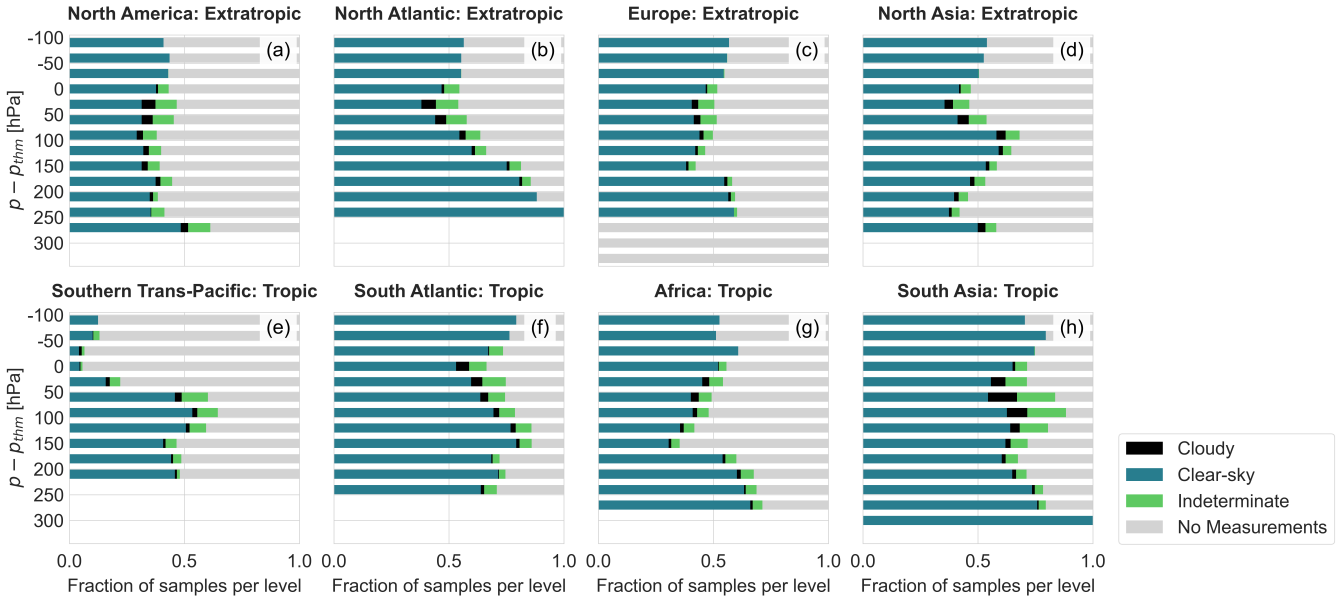

Figure 4. ~~(a-h)~~(a–h) Fraction of cloudy, clear-sky and indeterminate conditions per layer and region, based on the definitions using the cloud cover from ERA5. No measurements means that there is no data available on the ice crystal number concentration from IAGOS, which are flagged in the ERA5 dataset as well.

~~The mean annual global cirrus cloud occurrence using IAGOS measurements can be seen in Fig. 5. The location of large amounts of cirrus corresponds well with cirrus hotspots identified by Petzold et al. (2017), albeit the percentages are lower. This may be the result of using a larger timeframe compared to Petzold et al. (2017) given that we use the same discretisation for the figure. Similar percentages are achieved when considering the overall relative cirrus occurrence.~~

~~**Figure 5.** Mean annual cirrus cloud occurrence using IAGOS number of ice particles for all considered vertical levels and measurements between July 2011 and December 2022. Light grey area is the entire coverage of the IAGOS flights considered in this study, for which there are no measurements for number of ice particles.~~

2.5 ~~North Atlantic weather pattern classification~~

The North Atlantic weather patterns are determined using the classification presented by Irvine et al. (2013), which is based on the similarity of the daily mean geopotential height anomaly to typical patterns, i.e. the North Atlantic Oscillation (NAO) and East Atlantic (EA) patterns. The daily mean geopotential height is obtained from the Copernicus Climate Data Store (CDS) (Hersbach et al., 2023b) at a pressure level of 250 hPa. Subsequently, the anomalies with respect to the entire period 2011-2022 are calculated. Days are then assigned to five winter weather patterns (W1-W5) and three summer weather patterns (S1-S3), according to a set of criteria (Irvine et al., 2013). The characteristics of these weather patterns can be found in Table 4. The frequency of these patterns is presented in Fig. 6. The average number of days per season within each weather pattern class aligns well with the literature (Irvine et al., 2013). The analysis in Sect. 3.6 considers the extended winter season, from December to March.

Table 4. North Atlantic weather pattern characteristics for winter (W1-W5) and summer (S1-S3) (Irvine et al., 2013).

Figure 6. Frequency of **a)** winter weather patterns and **b)** summer weather patterns per year (2011-2022) using ERA5.

3 Results

The aim of this section is to compare temperature, RHi and ISSR occurrence between IAGOS and ERA5.

3.1 Seasonal and vertical variability of temperature between ERA5 and IAGOS

3.1 Distribution of temperature from IAGOS and ERA5

As a first step, we compare the IAGOS measured temperature and the ERA5 simulated temperature. This is important to consider, as relative humidity partially depends on temperature (Reutter et al., 2020). Figure 7 Figure 5 shows the vertical mean temperature distribution of IAGOS and ERA5 per season, for the eight geographical regions defined. The choice for the lower limit on the number of samples is explained in Sect. S1 S2 in the Supplement. Overall, there is good agreement in temperature, though ERA5 tends to have a cold bias in the extratropics, both in the upper troposphere and lower stratosphere. This is in line with results presented by Wolf et al. (2025) for mid-latitudes at different pressure levels. The cold bias observed in the upper troposphere may be due to sensor error as the mean difference, around 0.5 K, is within the accuracy of the IAGOS temperature sensor, as can be observed in Fig. S5 in the Supplement. Here, it can also be seen that the lower stratosphere shows a slightly larger cold bias compared to the upper troposphere, with mean differences ranging from 0.75 K to 1 K and can thus not be explained by sensor accuracy alone. Shepherd et al. (2018) also reported a cold bias of up to 0.5 K in comparison to radiosondes in the lower stratosphere of ERA5 due to an underlying cold bias in the IFS.

also shows the extratropical seasonal cycle in temperature, with higher temperatures found in JJA and lower temperatures in DJF. However, temperature differences between IAGOS and ERA5 show no seasonal cycle, with similar mean differences observed between all four seasons, as seen in Fig. S5 in the Supplement. In North Asia, ERA5 shows a warm bias for season DJF until approximately 60 hPa below the tropopause, after which the mean difference approaches that of the other seasons. In the lower stratosphere, season DJF again starts to deviate from the other seasons, with the mean difference decreasing until

ERA5 shows a warm bias again. However, given the mean differences are within the sensor accuracy of IAGOS, sensor error cannot be ruled out.

Meanwhile, the tropical regions show a better approximation of the temperature in ERA5 below the tropopause. The mean temperature differences

The mean temperature differences in the tropical regions range between -0.25 K (ERA5 warmer than IAGOS) and 0.25 K, on average, in the upper troposphere . This as observed in Fig. S11 in the supplement, which is within the IAGOS temperature sensor accuracy range. In Africa, we see mean temperature differences between 0.5 K and 1 K. Furthermore, the tropics show an increased deviation between IAGOS and ERA5 close to and above the tropopause. In South Asia and Africa, the deviation causes a cold bias in ERA5, which can be attributed to the stratospheric cold bias in ERA5 (Shepherd et al., 2018). However, in the Southern Trans-Pacific, the increased deviation results in a warm bias, which may be partially explained by sensor error. Generally, the minimum temperature is found at the thermal tropopause (Hoffmann and Spang, 2022), but in South Asia for season JJA, the minimum temperature is found approximately 60 hPa below the thermal tropopause. We conclude

In the extratropics, we find that ERA5 has a cold bias of 0.5 K on average in the upper troposphere, but it cannot be ruled out that this is not due to the following reasons as their consideration still results in the minimum temperature being located 30 hPa below the tropopause: the calculation of the tropopause or the temperature field in ERA5, outliers for specific years, and low sampling at the tropopause and in the lower stratosphere between 20S and 20N. We also find that the minimum temperature occurs at the same distance from the dynamic tropopause. Hence, we hypothesise it may be due to the type of weather encountered in season JJA in South Asia as deep convection can lead to perturbation of the temperature profiles with respect to altitude (Muhsin et al., 2018). sensor error as the mean difference is within accuracy range of the IAGOS temperature sensor. The lower stratosphere shows a slightly larger cold bias compared to the upper troposphere, with mean differences ranging from 0.75 K to 1 K and can thus not be explained by sensor accuracy alone.

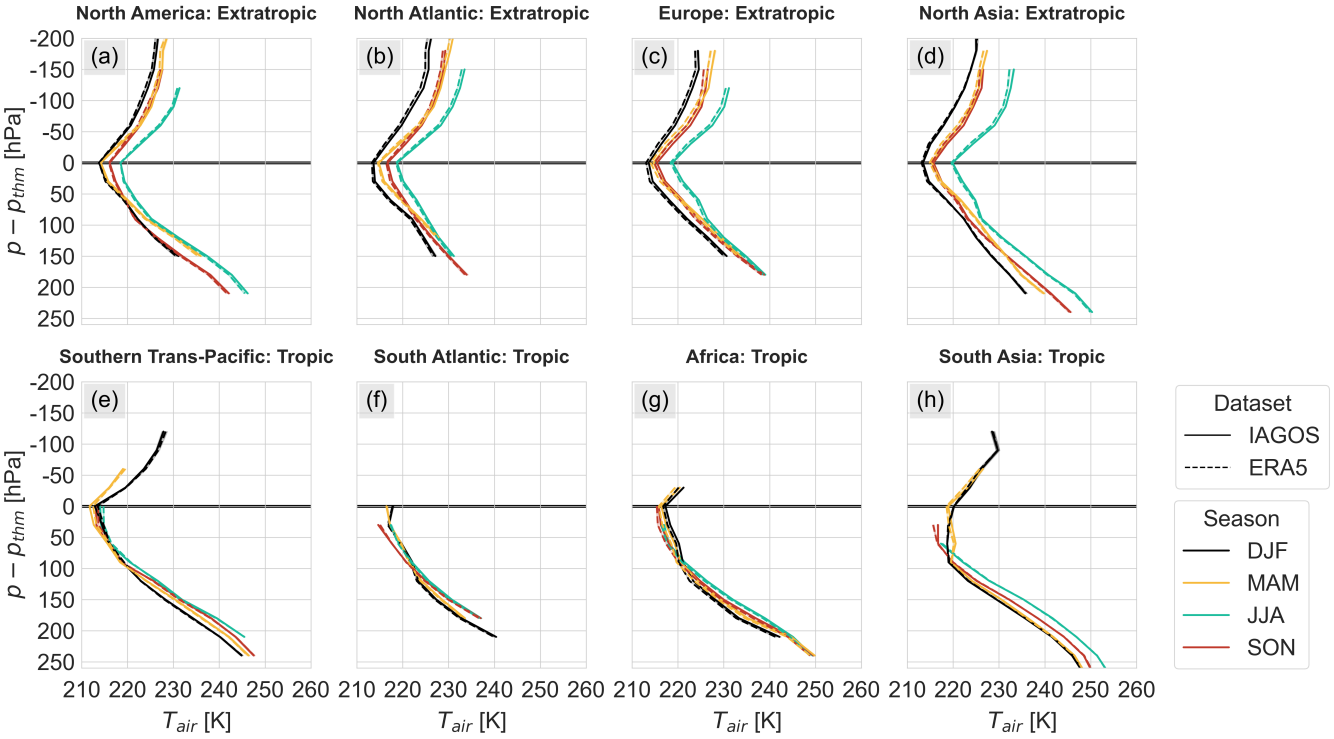

Figure 5. (a–h)Vertical distribution of IAGOS and ERA5 mean temperature per season and per region with shading showing the 95% confidence interval, using levels based on distance to thermal tropopause, only considering levels, seasons and regions with 500+ samples.

3.2 ~~Distribution~~ Seasonal and vertical variability of relative humidity over ice ~~from IAGOS and~~ between ERA5 and IAGOS

Ice supersaturation is governed by the RHi. We only consider RHi for cases where the temperature is below the threshold of homogeneous freezing, assumed equal to 235.15 K. This is the lowest temperature at which supercooling of cloud droplets can occur (Gierens et al., 2020b; Sperber and Gierens, 2023). Less than 5% of our IAGOS measurements show ISS above this temperature threshold.

~~Figure 8 shows a two-dimensional histogram, illustrating the overall ability of ERA5 to predict RHi. It shows a high frequency of points along the perfect agreement line. However, the highest frequency along this line occurs at low values of RHi, which shows that ERA5 is more accurate at low values, as has also been observed by Wolf et al. (2025). There is also a high frequency of points along the RHi (ERA5) = 1 line due to the saturation adjustment in ERA5, in which the RHi is adjusted back to one when supersaturation occurs in a cloudy grid box, causing a concentration around this value. This is similar to the results obtained by Gierens et al. (2020a), Wolf et al. (2025), and Wang et al. (2025).~~

~~**Figure 8.** Two-dimensional histogram of ERA5 relative humidity over ice as a function of IAGOS relative humidity of ice.~~

The mean vertical ~~RHi of~~ distribution of RHi in the IAGOS and ERA5 datasets per season and geographic region is presented in Fig. ~~9. Generally, ERA5 shows a dry bias, both in the upper troposphere and in the lower stratosphere. This is in line with other studies, such as Reutter et al. (2020) and Wolf et al. (2025). Some studies have reported a general moist bias in the lower stratosphere in the ECMWF-IFS (Dyroff et al., 2014; Shepherd et al., 2018; Bland et al., 2021), but we observe that the mean IAGOS RHi is higher than the mean ERA5 RHi in the lower stratosphere. However, we cannot ascertain that this is due to biases in ERA5. As explained by Wolf et al. (2025), low values of RHi measured by IAGOS in the lower stratosphere are subject to a moist bias. This results from the limitation of the ICH sensor; it does not provide good quality results in dry conditions due to the loss of sensitivity as a result of the adiabatic compression effect (Konjari et al., 2025).~~

~~In the lower stratosphere, the range of RHi differences between IAGOS and ERA5 is smaller compared to the upper troposphere, as displayed in Fig. S6 in the Supplement. This is~~ 6. In the tropics, we observe some seasonal behaviour in the Southern Trans-Pacific and in South Asia. South Asia has a larger mean RHi in season JJA compared to the other seasons in this region. The higher RHi may be the result of the tropics being a deep-convection region with strong updrafts, which result in ISS and high nucleation rates leading to a high ice crystal number concentration (Sanogo et al., 2024). Petzold et al. (2017) also found a correlation between a high ice crystal number concentration and high values of RHi. In fact, we find a higher frequency of cloudy conditions for season JJA compared to other seasons in South Asia when observing IAGOS measurements (see Fig. S13), showing that more measurements with larger ice crystal number concentrations are found in this season. Although deep convection can also happen in other tropical regions, we do not observe this due to the ~~dryness of the lower stratosphere, resulting in lower values of RHi as seen by the rapid decrease of RHi from approximately 30 hPa below the tropopause~~ low sampling of in-cloud measurements with IAGOS in these regions.

For season JJA in South Asia, we also identify a moist bias in ERA5. Schneider et al. (2014) showed that the latitudinal band of 0 to 30~~hPa above the tropopause, which then changes to a near-vertical asymptote. This is more apparent in the extratropics, as the tropopause in the tropics is located at a higher altitude, which causes fewer samples in the lower stratosphere. Petzold et al. (2020) found the same vertical distribution of~~ ° N, for a region covering 65° E to 95° E, received the most precipitation in JJA, including September. Hence, we suggest that the moist bias may be related to the type of weather encountered in South Asia in season JJA.

In the Southern Trans-Pacific, season DJF shows an overall lower mean RHi compared to other seasons. The majority of points in this region are located close to Hawaii or Central America/northwestern South America. Based on the correlation between RHi and cloud ice particles, the lower RHi ~~with respect to tropopause layers in extratropic regions. The lower values of RHi results in ERA5 finding values of RHi closer to what has been observed with IAGOS. This was also shown in Fig. 8 with the large concentration of points along the perfect agreement line at low values of RHi . However, we acknowledge the possibility of a moist bias in IAGOS, which means that ERA5 may show better ability of predicting RHi in the lower stratosphere than the results shown.~~ could be related to little to no cloudy conditions in DJF (see Fig. S13).

~~The seasonal behaviour of RHi is more apparent in the extratropics compared to the tropics.~~ In North America, North Atlantic, and Europe, the highest RHi ~~is observed for~~ values throughout the vertical profile occur during seasons DJF and MAM, which are also the seasons that exhibit the ~~seasons with the~~ lowest mean temperatures, as seen in ~~Fig~~as seen in Fig.

5. 7. These are also the two seasons where we find a larger dry bias in ERA5. This is due to higher values of RHi favouring lower temperatures (Sanogo et al., 2024), and ERA5 shows more inconsistencies in the prediction of large RHi as shown in Fig. 6 and by Wolf et al. (2025). It is also interesting to note that these differences (Wolf et al., 2025). We also find that the differences between IAGOS and ERA5 appear smallest in North America and increase as we move towards Europe, showing a possible longitudinal dependency. This was also observed by Wolf et al. (2025) , who Wolf et al. (2025) noticed the same behaviour and hypothesised it could due to the spatial distribution of water vapour. From a global distribution of the mean RHi and ISS occurrence using IAGOS, we see that North America is drier, with less ISS occurrences, compared to the North Atlantic and Europe, which could result in larger differences in the two latter regions due larger biases in ERA5 close to and in ISS conditions (Petzold et al., 2020; Wolf et al., 2025). Just below the tropopause and in the

In the lower stratosphere, the seasonality of RHi disappears, as also shown by Petzold et al. (2020).

While we do not observe a seasonal cycle in RHi in the tropics, we do find that South Asia has a larger mean RHi in season JJA there is a larger difference in the mean RHi between IAGOS and ERA5 compared to the other seasons in this region. The higher RHi may be the result of the tropics being a deep-convection region with strong updrafts, which result in ISS and high nucleation rates leading to a high number of ice particles (Sanogo et al., 2024). Petzold et al. (2017) also found a correlation between a high number of ice particles and high upper troposphere, which can also be seen in Fig. S12 in the supplement. This reflects the moist bias in IAGOS at low values of RHi . In fact, we find a higher frequency of cloudy conditions for season JJA compared to other seasons in South Asia when observing IAGOS measurements, showing that more measurements with larger number of ice particles are found in this season. Interestingly, for season JJA in South Asia, we also identify a moist bias in ERA5. This is also the same region and season for which the minimum temperature did not coincide with the location of the thermal tropopause. Hence, we theorise that the moist bias may also be related to the type of weather encountered in South Asia in season JJA.

Overall, the expected differences in RHi in the dry lower stratosphere (Wolf et al., 2025). This results from the limitation of the ICH sensor; it does not provide good quality results in dry conditions in the lower stratosphere due to the loss of sensitivity as a result of the adiabatic compression effect (Konjari et al., 2025). Although the mean difference is larger in the lower stratosphere, Fig. S12 shows that the range of differences is smaller compared to the upper troposphere. This indicates that under conditions where RHi is lower, there is better agreement between IAGOS and ERA5are not governed by the location relative to the local tropopause, but rather by the atmospheric layer, i.e. upper tropopause or lower stratosphere. The largest biases in ERA5 are expected in the upper troposphere, with a tendency for ERA5 to be drier than IAGOS . Moreover, in the extratropics, colder months tend to result in a larger dry bias in ERA5, but the systematic moist bias in IAGOS increases the mean difference.

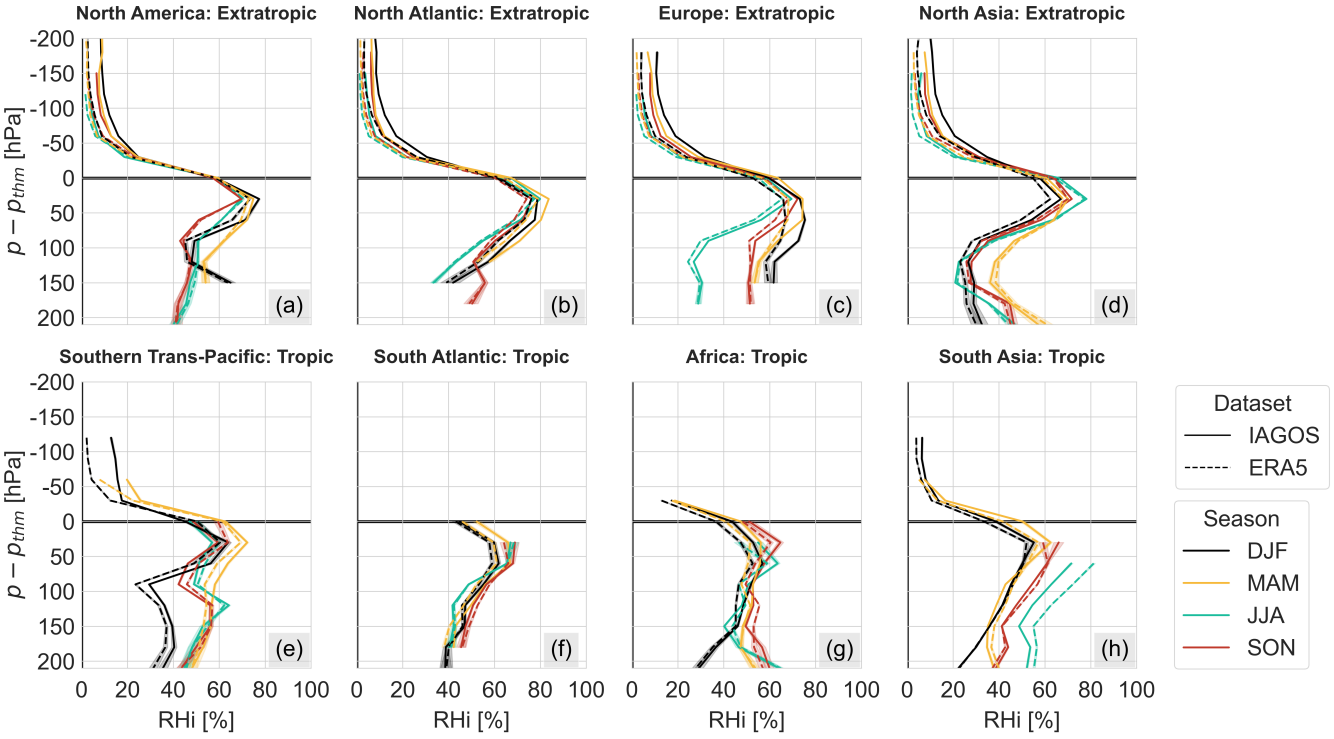

Figure 6. **(a–h)** Vertical distribution of IAGOS and ERA5 mean relative humidity over ice per season and per region with shading showing the 95% confidence interval, using levels based on distance to thermal tropopause, only considering levels, seasons and regions with 500+ samples.

3.3 Distribution of relative humidity over ice from IAGOS and ERA5 under cloudy and clear-sky conditions

In this section, we investigate the effect of clear-sky, indeterminate, and cloudy conditions based on the probability density function of RHi from IAGOS and ERA5. Instead of discrete vertical levels, we consider ~~the~~ three atmospheric layers because of the low sampling of the ~~number of ice particles~~ ice crystal number concentration in IAGOS. The three layers are upper troposphere (UT), tropopause (TROP) and lower stratosphere (LS). Their definition is based on the distance to the thermal tropopause ($p - p_{thm}$). The UT is defined as ~~$p_{thm} > 15$~~ $(p - p_{thm}) > 15$ hPa, the TROP as -15 hPa ~~$\leq p_{thm} \leq 15$~~ $\leq (p - p_{thm}) \leq 15$ hPa and LS as ~~$p_{thm} < -15$ hPa.~~ $(p - p_{thm}) < -15$ hPa. Note that for this analysis we consider conditions with 250+ samples instead of 500+ samples due to less measurements with ice crystal number concentration within IAGOS. However, as seen in Sect. S2 in the supplement, 250+ samples should still be sufficient.

Figure ~~10~~ 7 and Fig. ~~11~~ 8 display the probability density function (PDF) for the different cloudy conditions, per atmospheric layer, and per geographic region considered in this study. In the ~~lower stratosphere, we mainly observe the~~ LS, we find that the extratropic clear-sky PDF ~~of RHi due to rare cloud occurrence in this atmospheric layer. The clear-sky PDF~~ is governed by low values of RHi and ~~low probability of ISS, with~~ a general monotonically decreasing behaviour. ~~This was reported by~~

Gierens et al. (1999) using the global distribution of MOZAIC flights and it was also seen by Sanogo et al. (2024) for the lower stratosphere in high-latitude regions (60-80N) using IAGOS measurementsThe IAGOS measurements show that ISS is possible in the LS, but the probability of occurrence is low. Meanwhile, ERA5 shows little to no ISS occurrence under clear skies in the extratropics. In the tropic regions, the clear-sky PDF in the LS shows some multimodal behaviour, but this is most likely the result of a small number of samples in this atmospheric layer due to the high altitude of the tropopause in these regions (see Fig. 2). Here, the probability of ISS conditions is much more rare compared to the extratropics. However, we do observe a low probability of ISS conditions in South Asia.

Both the extratropics and tropics show small differences in low values of RHi in the LS under clear-sky conditions. This is not necessarily due to biases in ERA5, but may be due to limitations of the IAGOS ICH sensor as discussed in Sect. 3.2. However, this will not impact the prediction of ice supersaturated regions as the issue only arises below RHL $\approx 10\%$ (Konjari et al., 2025) , which is equivalent to RHi $\approx$ 15-1815–18% given the mean temperature in the LS.

The tropopause layer is not completely dry (Petzold et al., 2020; Reutter et al., 2020), hence we observe that ISS is possible in clear-sky, cloudy and indeterminate conditions, as shown in Fig. 10 and Fig. 11. As is evident from the comparison of the IAGOS and UT has more moisture compared to the TROP and LS, allowing for higher probabilities of ISS occurrence. However, the TROP also shows high ISS occurrence, both in the tropics and extratropics. This is in line with Reutter et al. (2020) , where it was found that there was a significant amount of in situ and ERA-interim data that exceeded the RHi = 100% threshold near the tropopause in the North Atlantic flight corridor. For UT and TROP clear-sky conditions, the probability of RHi > 100% is higher and there is a more uniform probability across the observed RHi range compared to the LS. ERA5 PDF, ERA5 shows good approximation of RHi below ISS in UT and TROP clear-sky conditions until RHi $\approx 0.75 - 0.90 \approx$ 75%–90%, with a lower probability of values greater than 1 compared to IAGOSdrop-off in probability just before RHi $= 100\%$. The underestimation of ISS in ERA5 for clear-sky conditions may be the result of the resolution of ERA5, which only provides hourly mean and grid cell values (Schumann et al., 2021). However, it shows that by lowering the threshold value of RHi for ISS, we could artificially increase the prediction of ISS in ERA5, though the value may differ per region; as seen from Fig. 107, the RHi threshold value would be close to 1 100% for North America, but it might be closer to 0.75 75% in Europe. On the other hand, indeterminate and cloudy conditions

Cloudy and indeterminate conditions in ERA5 for the UT and TROP are governed by peaks at RHi = 1 for ERA5, which is due to narrow peaks centred around RHi $= 100\%$ due to the saturation adjustment. For IAGOS, we also observe peaks for these conditions, but their distributions are wider and these peaks are centred at higher values of RHi, with wider distributions as cirrus clouds often exhibit an ice supersaturated wet mode, but they can also be subsaturated (Sanogo et al., 2024). Similar behaviour was observed by Wolf et al. (2025).

The upper troposphere has more moisture compared to the tropopause and lower stratosphere, allowing for higher probabilities of ISS occurrence. For clear-sky conditions, there is a smaller probability of low RHi, with increased probability of higher RHi, and a more equal probability across all observed RHi values. ERA5 shows a drop-off in probability just before RHi = 1, as was also seen in the tropopause. Again, this underestimation in ISS occurrence could be corrected by lowering the RHi threshold value for ISS in ERA5. Cloudy and indeterminate conditions in ERA5 for the UT are also governed by peaks centred

around RHi = 1, but with higher probabilities due to larger occurrences of these two conditions than at the TROP (see Fig. 4). As seen at the TROP, IAGOS is centered at values of RHi just above 1 in the UT for these two conditions, with higher probabilities. Again, the overall behaviour is similar to that found by Wolf et al. (2025), but we find larger difference in the peak probability between IAGOS and ERA5 for cloudy and indeterminate conditions, which may be the result of taking into account the different atmospheric layers. If we consider the same geographic area, pressure levels and time frame for IAGOS measurements as Wolf et al. (2025) and do not consider separate atmospheric layers and do not normalise given the number of observations, we obtain more similar results to Wolf et al. (2025). This shows that the atmospheric layer plays a role in the behaviour of the PDF.

Comparison of extratropic and tropic PDFs for cloudy and indeterminate conditions, shows similar behaviour. However, in South Asia, In South Asia, we find that this mode is located at values lower than 1, i.e. it is subsaturated . Sanogo et al. (2024) found similar observations when considering a larger tropical region. While we do not find this observation in the other tropic regions, it makes sense that Sanogo et al. (2024) finds this overall observation due to the high percentage of measurements in the South Asia regionsubsaturated in the UT in the IAGOS measurements. This observation in South Asia may also provide insights into the moist bias found in JJA (Sect. 3.2). The mean vertical distribution of RHi shows a higher mean RHi for ERA5 compared to IAGOS in cloudy and indeterminate conditions for South Asia in JJA, at vertical levels below the tropopause. This is because the mean RHi in IAGOS for this particular region and season is less than 1 100% in cloudy and indeterminate conditions, which is inline aligns with the behaviour of the RHi PDF, whereas ERA5 shows a mean of 1 due to the saturation adjustment100%. Therefore, the moist bias appears to arise as a result of the saturation adjustment, which because ERA5 cannot take into account that the (wet) mode of the RHi PDF wet mode in cloudy conditions can be subsaturated in some regions. Whether the subsaturation is a result of the specific season in weather conditions in JJA in South Asia is uncertain and requires further evaluation.

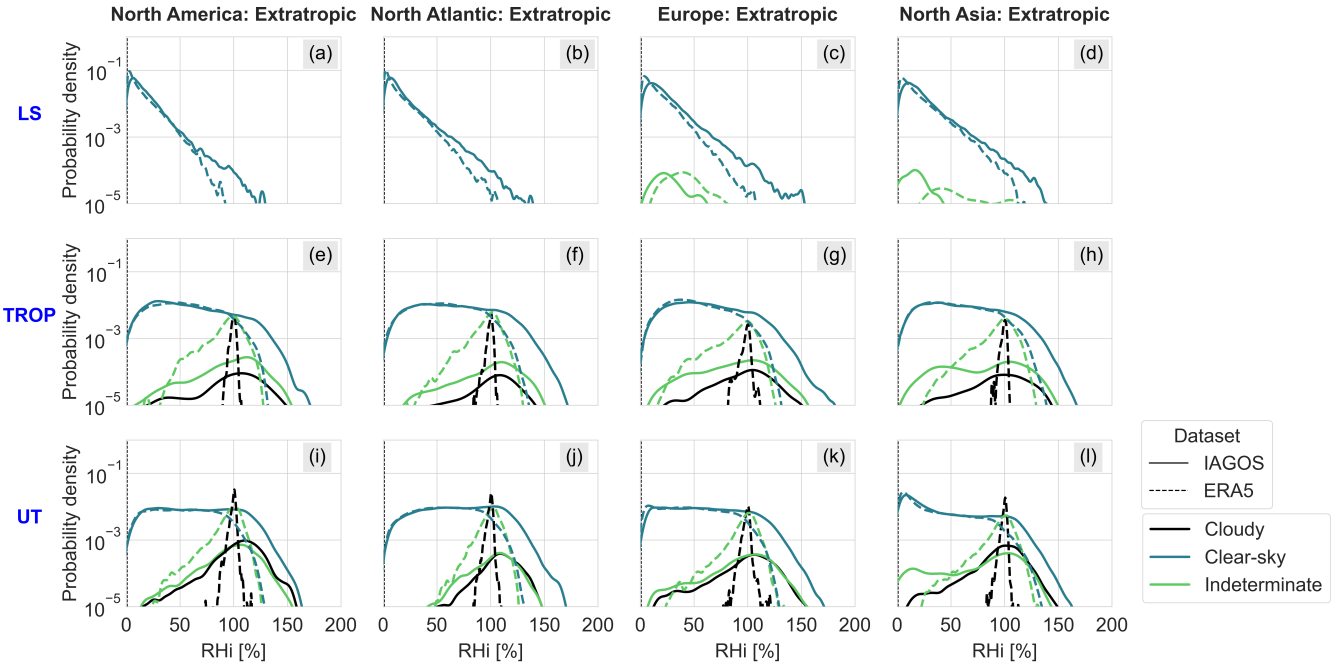

Figure 7. ~~(a–l)~~ (a–l) Probability density function of IAGOS and ERA5 relative humidity over ice in the upper troposphere (UT), at the tropopause (TROP) and in the lower stratosphere (LS) for cloudy, clear-sky and indeterminate conditions in the four extratropic regions. The PDFs per subplot are normalised with respect to the number of observations within each subset of IAGOS or ERA5 used for that subplot. Only regions and atmospheric layers with 250+ samples are considered.

~~Overall, ERA5 tends to estimate RHi well in clear-sky conditions, until just before ISS, but underestimates RHi in ISS conditions. Hence, for clear-sky conditions, we can expect an underestimation of ISSRs, but this could be improved by lowering the threshold value of RHi for ISS. However, in cloudy and indeterminate conditions, ERA5 shows narrow RHi distributions centred at 1 due to the saturation adjustment, while IAGOS shows that higher values can occur in such conditions. As a result of this, ERA5 may predict less ISSRs compared to ERA5. IAGOS also shows that some regions, such as South Asia, can have a subsaturated wet mode in cloudy and indeterminate conditions that ERA5 cannot predict due to the saturation adjustment. This may lead to an overestimation of ISSRs in ERA5.~~

3.4 Distribution of ice supersaturated regions in ~~IAGOS and~~ ERA5 and IAGOS

Comparison of the RHi showed a general dry bias in ERA5, compared to IAGOS, with some seasonal and regional differences. In the following section, we will explore the impact of such biases on the ice supersaturated region occurrence.

Figure ~~12~~ 9 displays the vertical distribution of the ISSR fraction per season and geographical region. The ISSR fraction is calculated by finding the total number of points showing ISS conditions and dividing by the total number of points, per vertical level, season and geographical region. There is an overall underestimation of ISSRs in ERA5 due to the dry bias in RHi. ~~This was also reported by Reutter et al. (2020) when considering the North Atlantic region.~~ In instances where the RHi is overesti-

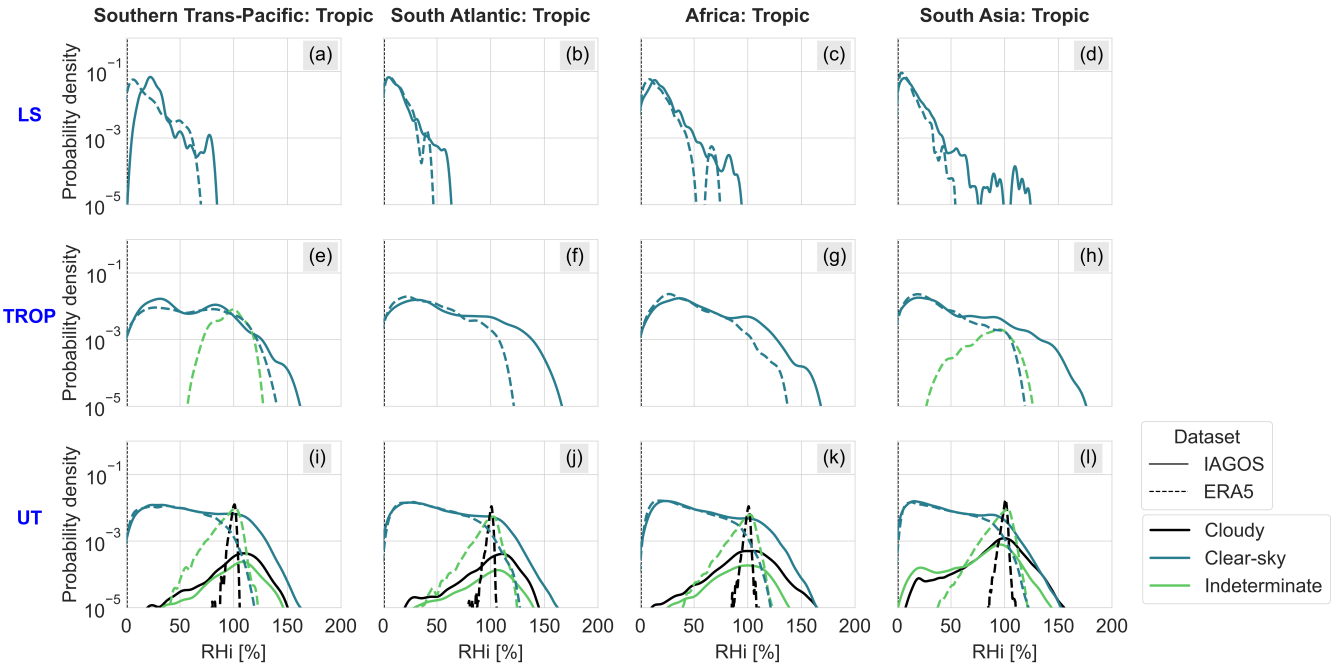

Figure 8. ~~(a-l)~~ (a–l) Probability density function of IAGOS and ERA5 relative humidity over ice in the upper troposphere (UT), at the tropopause (TROP) and in the lower stratosphere (LS) for cloudy, clear-sky and indeterminate conditions in the four tropic regions. The PDFs per subplot are normalised with respect to the number of observations within each subset of IAGOS or ERA5 used for that subplot. Only regions and atmospheric layers with 250+ samples are considered.

mated by ERA5, such as in South Asia for season JJA, the ISSR fraction is overestimated by ERA5. ~~Agarwal et al. (2022) finds a tendency for ERA5 to overestimate the ISSR occurrence at cruise altitudes in the tropicsand mid-latitudes when compared to radiosonde measurements. However, the radiosonde measurements are not corrected for dry biases and the location of these radiosonde observations are generally over land and not very widespread as with the IAGOS measurements, which could lead to differences in obtained results.~~

~~From a seasonal perspective, there is a clear seasonal pattern in North America, North Atlanticand Europe, with seasons DJF and MAM showing highest ISSR occurrence. This is in line with other research, such as done by Petzold et al. (2020) and Sanogo et al. (2024). However, we do not find a distinct seasonal behaviour in the tropics, just as with the relative humidity over ice. This is also in line with Sanogo et al. (2024), who found the ISSR frequency to vary by around 5% or less among the four considered seasons in the tropics.~~

~~We find~~ In the tropics, we generally report an increasing ISSR fraction up to just below the tropopause, with a maximum of 20%. The South Atlantic, Africa, and South Asia show little seasonal dependence. In the Southern Trans-Pacific, it is observed that the maximum ISSR fraction in the ~~extratropic regions is between 30~~ Southern Trans-Pacific occurs closer to the tropopause in DJF than in JJA. The vertical profile of the mean RHi in DJF for this region also showed a more pronounced increase near

the tropopause compared to other seasons (see Fig. 6). In the layer between 100 hPa and ~~35% for seasons DJF or MAM using IAGOS measurements. The maximum ISSR fraction occurs just below the tropopause, around 30 hPa (approximately 750 m at cruise level) (Thouret et al., 2006; Petzold et al., 2020) and reduces to zero in the lower stratosphere. This is similar to what was reported by Petzold et al. (2020). On the other hand, Reutter et al. (2020) found a maximum of 40% using IAGOS when considering all seasons , but with the maximum also occurring 30 hPa~~ 200 hPa below the tropopause~~and a reduction of ,~~ the ISSR fraction ~~to zero in the lower stratosphere. Sanogo et al. (2024) found a maximum ISSR frequency of around 20% in the mid-latitudes for seasonsMAM and DJF. However,~~ in DJF is lower than in the other seasons, which is consistent with the lower mean RHi in this layer.

For South Asia, we do not find that the ISSR fraction is ~~highly sensitive to the number of points available and these studies use a different subset of the IAGOS /MOZAIC dataset. In the tropics, we report an increasing ISSR fraction until just below the tropopause, with a maximum of approximately 20%, but is independent of the season. Sanogo et al. (2024) reports a maximum ISSR fraction of 15% in~~ higher in JJA in the IAGOS measurements, despite the higher overall mean RHi. This could be related to the higher frequency of cloudy conditions in South Asia in JJA, for which the wet mode of the ~~tropics using IAGOS and with no seasonal variation. The ISSR fraction also increases with altitude for pressure levels below the average thermal tropopause height~~ RHi PDF is subsaturated, leading to less ISS occurrences. ERA5 shows a higher ISSR fraction throughout the vertical profile in JJA; this was also the season for which ERA5 showed a moist bias. Otherwise, we find no distinct seasonal behaviour in the tropics. ~~Lamquin et al. (2012) also showed increasing ISSR occurrence with altitude in the tropics using MOZAIC, with maximum ISSR frequencies of up to~~

There is a clear seasonal pattern in North America, North Atlantic and Europe, with DJF and MAM showing the highest ISSR occurrence. For these seasons, IAGOS shows maximum ISSR fractions between 30% ~~, but this study considered the frequency per grid box and not an overall defined region~~and 35% with IAGOS, typically occurring just below the tropopause (around 30 hPa, $\approx$ 750 m at cruise level; Thouret et al. (2006); Petzold et al. (2020)) and decreases to zero in the lower stratosphere.

To quantify the skill of ERA5 in predicting ISSRs, we can use the equitable threat score (ETS). This performance measure is preferred over measures such as the hit rate and false alarm rate since ISSRs can be a rare event (Gierens et al., 2020a; Wolf et al., 2025), for example in the lower stratosphere. The ETS is calculated using Eq. 1, where r is found with Eq. 2 and the other variables are entries in the contingency table shown in Table 4. If ETS $= 1$, ~~it means that~~ there is a perfect correlation between the observation and the prediction (Gierens et al., 2020a). When ETS $= 0$, ~~it means that~~ the relationship is completely random (Gierens et al., 2020a). We investigate how the ETS varies with different RHi thresholds in ERA5, while keeping the threshold of 100% in IAGOS.

$$\mathrm{ETS} = \frac{\mathrm{TP} - r}{\mathrm{TP} + \mathrm{FN} + \mathrm{FP} - r} \tag{1}$$

$$r = \frac{(\mathrm{TP} + \mathrm{FN})(\mathrm{TP} + \mathrm{FP})}{\mathrm{TP} + \mathrm{FN} + \mathrm{FP} + \mathrm{TN}} \tag{2}$$

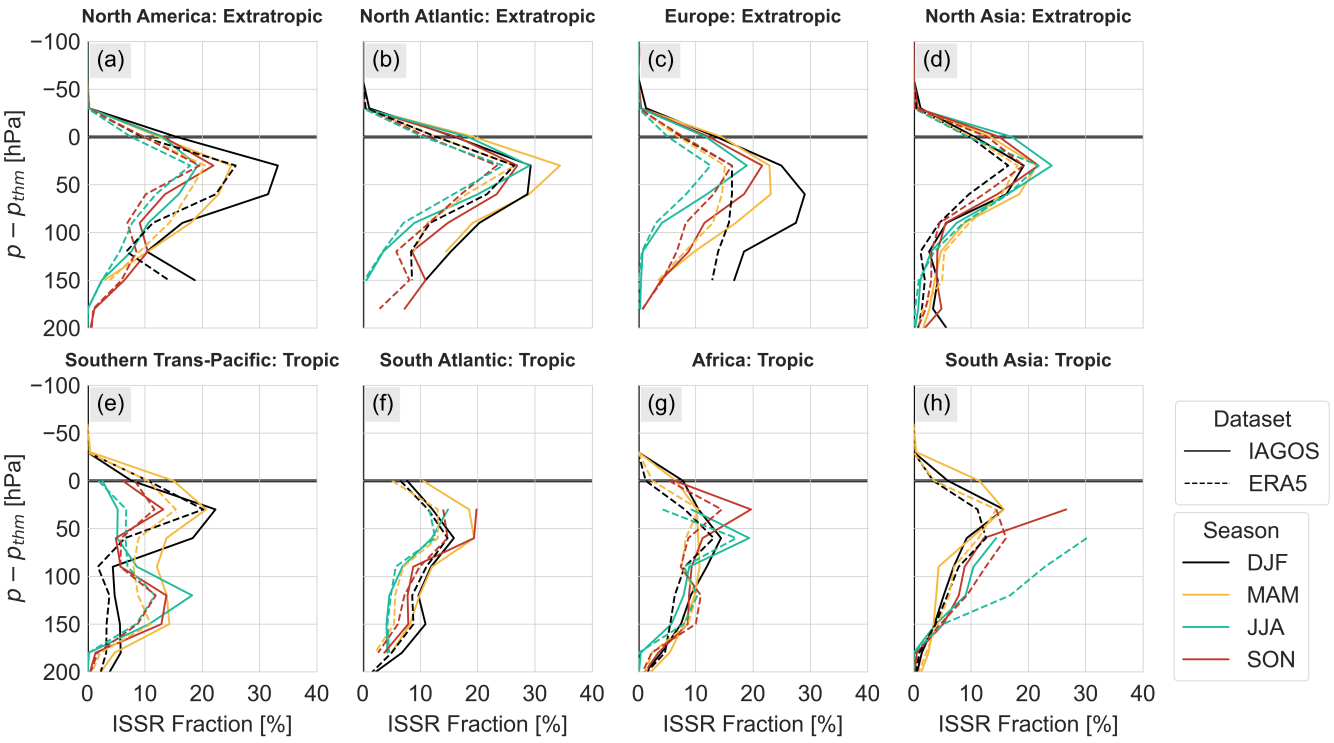

Figure 9. ~~(a–h)~~ (a–h) Vertical distribution of IAGOS and ERA5 ice supersaturated region fraction per season and geographical region. Only ~~consider~~ levels, seasons and regions with 500+ samples are considered.

Table 4. Contingency table definition.

IAGOS observation	**ERA5 prediction**	
	Yes	No
Yes	True positive (TP)	False negative (FN)
No	False positive (FP)	True negative (TN)

Figure ~~13~~ 10 and 11 shows the vertical distribution of the ETS per ~~season and geographical region . Overall~~geographical region for different ERA5 RHi thresholds in DJF and JJA, respectively. When using the threshold of RHi = 100%, the ETS lies between 0.2 and 0.4 in the upper troposphere, depending on the season, vertical distance to the tropopause and region. This means that there is a weak to mediocre correlation between IAGOS and ERA5 in the prediction of ISSRs. ~~The high ETS seen for North~~ There are a few instances of high ETS scores: North America in season JJA at 180 hPa below the tropopause and North Atlantic in season DJF at 150 hPa below the tropopause~~and for~~ . For North America in season JJA at ~~180 hPabelow the tropopause appear to be outliers, even though more than 500 samples have been used to calculate the ETS at these conditions~~

~~(see Sect. S1 in the Supplement). Otherwise, the ETS remains relatively constant with distance from the tropopause in the upper troposphere. It begins to decrease at the tropopause and reduces further in the lower stratosphere. We also find low ETS at 200 hPabelow the tropopause. Both in the lower stratosphere and well~~ $180 - p_{thm}$ hPa, there is a low number of ISSRs in both IAGOS and ERA5 (see Fig. 9), where one measurement point is classified as TP, one point as FN and the rest as TN. Since the ISSR events are rare, resulting in a perfect hit rate, accompanied with most points classified as TN, the ETS can inflate. We see a similar low ISSR fraction for North America in season JJA at $150 - p_{thm}$ hPa, although the ETS is not as high. This can be attributed to more points being categorised as FN and FP, lowering the ETS. In the North Atlantic, in season DJF at 150 hPa below the tropopause, ~~ISSR occurrence is rare (see Fig. 12). Hence,~~ we also find a high ETS. In the instances where an ISSR is observed here, most of these events are classified as TP, with no misses (FN = 0), and there were few points classified as FP compared to TP. At the same time, there are also many points classified as TN. The combination of this leads to a high ETS.

By reducing the RHi threshold, we can improve the ability of ERA5 ~~shows decreased ISSR predictive skills when its occurrence is rare. When the ETS is 0, such as 60 hPa above the tropopause in North America, it is the result of IAGOS not observing any ISSRs, but ERA5 predicting their occurrence, which results in ERA5 showing no skill. Gierens et al. (2020a) calculated ETS between 0.05 and 0.25, depending on the season. The value of 0.05 is on the lower side, but this may be because the study does not take into account the different atmospheric layers or regions, and also only considers four months of IAGOS measurements. If we do not take into account the vertical layers defined,~~ to predict ISSRs, as shown by the ETS. The optimal RHi thresholds are in the range of 85% to 95% in the upper troposphere and in the tropopause. However, it is also dependent on the region, distance from the tropopause and the ~~ETS remains between 0.15 and~~ season, but a clear pattern is difficult to establish. In the extratropics, more improvements in the ability of ERA5 to predict ISSRs can be achieved in DJF by reducing the RHi threshold compared to in JJA. This could be due to lower mean RHi values and thus ISSRs in warmer months, such as JJA, although North Asia shows the highest ISSR fraction for this season, as seen in Fig. 9. SON and MAM also show more improvements compared to JJA when lowering the RHi threshold (see Sect. S5 in the supplement). Overall, only a certain improvement can be achieved by changing the RHi threshold. Not accounting for the outliers, we observe that we cannot achieve an ETS higher than approximately 0.5 in DJF and around 0.3 ~~. Hence, the low ETS found by Gierens et al. (2020a) is most likely the result of using a smaller subset of IAGOS and~~ in JJA in the upper troposphere and in the tropopause.

In the extratropic lower stratosphere, lowering the RHi threshold in ERA5 ~~data. The study by Wang et al. (2025) shows an ETS of 0.23 upper troposphere (UT) and 0.14 in~~ shows some improvement in the ETS, but the ~~lower stratosphere before application of the machine learning algorithm, which agrees well with the values identified in this study.~~ ETS score still indicates a weak correlation between IAGOS and ERA5. There is a low number of ISSR occurrences in this layer, which combined with the underestimation of RHi in ISS conditions, might make it difficult for ERA5 to predict ISSRs in these instances. In North America and Europe, the best ETS at 30 hPa above tropopause was found at an RHi threshold of 75%; perhaps lowering the threshold even more could allow for more improvements.

~~From a regional perspective, we find a higher ETS in North America, which decreases as we move towards Europe. For these three regions, we also found a possible longitudinal dependency in the RHi difference, discussed in Sect. 3.2, where North America has the lowest difference and Europe the highest. Hence, the lower RHi difference leads to a higher ETS,~~

~~showing better ISSR prediction skills in ERA5.~~ In the tropics, ~~the ETS is lower than in the extratropics at most vertical levels defined. At 30 hPa below the tropopause, the ETS increases, but the reason is unknown given that we tend find larger differences in RHi for these distances from the tropopause. On the other hand,~~ DJF also shows larger ETS improvements by decreasing the RHi threshold compared to other seasons in the upper tropopshere. It is also interesting to note than in South Asia in ~~season JJAhas one of the lowest ETS, which is the result of the moist bias seen in Sect. 3.2, leading to more FPs in the prediction of ISSRs.~~

~~There is some seasonal variation in the ETS; the maximum difference between seasons is approximately 10%, at most. In North America~~JJA, where we observed a moist bias in ERA5, both increasing and decreasing the RHi threshold in ERA5 has little to no impact on the ETS. This could be the result of a higher frequency of cloudy conditions in this particular season, for which changing the RHi threshold may not have a large effect. In Southern Trans-Pacific, we find that ~~the variation can be up to 20%. Nevertheless, in the extratropics, we tend to find that season SON and DJF results in the highest ETS and season JJAand MAM in the lowest. Gierens et al. (2020a) also showed approximately 10% variation in the ETS between seasons, with the largest ETSoccurring in January (winter), equivalent to DJF, and lowest ETS in July (summer), equivalent to JJA. Hence, this shows that in the extratropics, we tend find a better agreement in the prediction of ISSRs between IAGOS and~~ ERA5 ~~for fall and winter. No specific seasonal trends are identified for the ETS in the tropics~~shows better prediction of ISSRs when lowering the RHi threshold in DJF, compared to in JJA, MAM and SON, with SON showing the lowest ETS. SON has the highest fraction of cloudy conditions and DJF the lowest. Perhaps cloudy conditions may be a limiting factor when decreasing the ERA5 RHi threshold to improve its ability to predict ISSRs, although we do not observe the same in the extratropics; this will be analysed further in the following section.

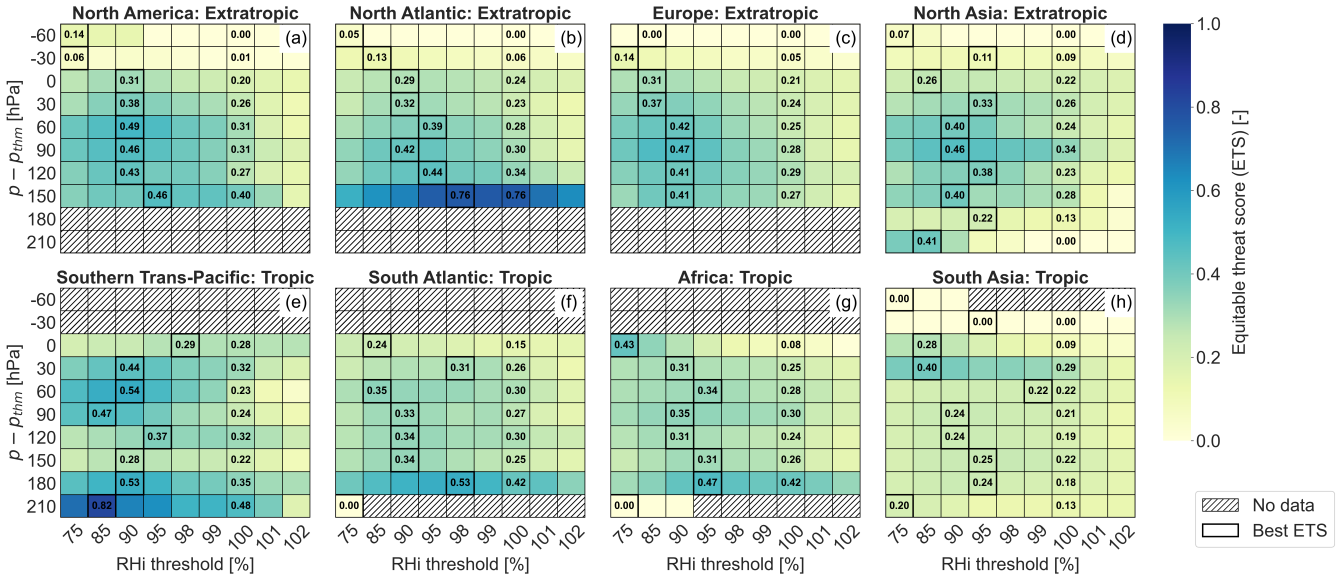

Figure 10. ~~(a–h)~~ (a–h) Vertical distribution of ice supersaturated region equitable threat score per ~~season and~~ geographical region for different ERA5 RHi thresholds in DJF. For each level, we highlight the ETS for a threshold of 100% and the ETS for the threshold at which we find the maximum value. ETS is calculated for level, season and region for which there are 500+ samples.

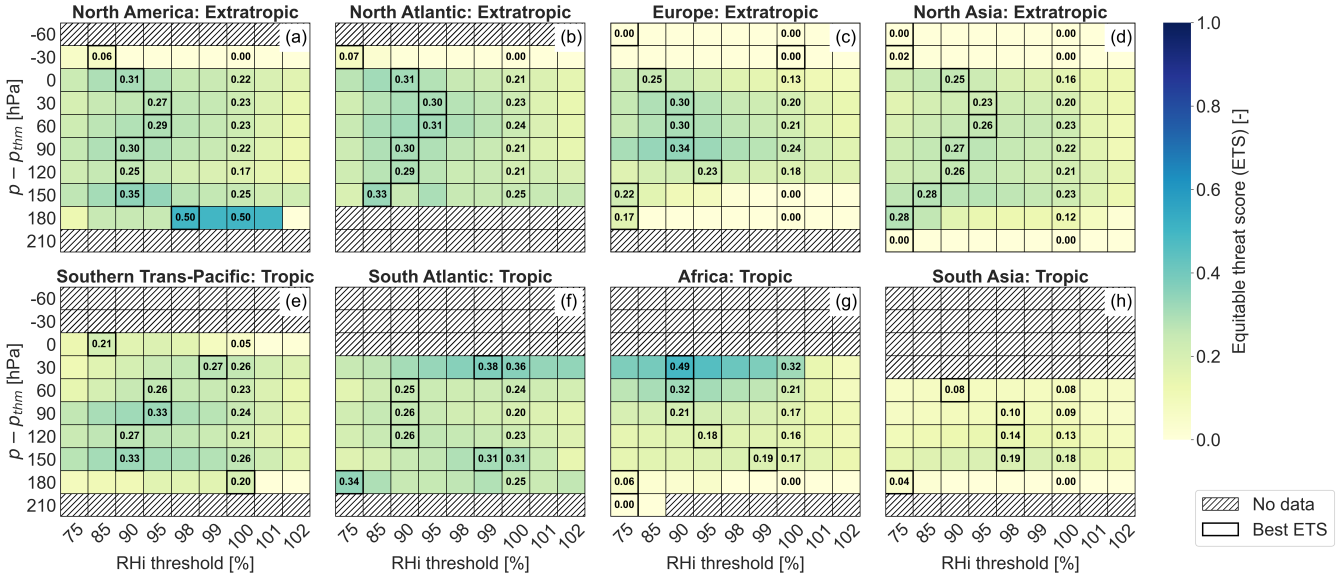

Figure 11. (a–h) Vertical distribution of ice supersaturated region equitable threat score per geographical region for different ERA5 RHi thresholds in JJA. For each level, we highlight the ETS for a threshold of 100% and the ETS for the threshold at which we find the maximum value. ETS is calculated for level, season and region for which there are 500+ samples.

3.5 Prediction of ice supersaturated regions in ERA5 under cloudy and clear-sky conditions

In Sect. 3.3, the effect of cloudy conditions on the RHi was investigated for the different atmospheric layers and for the different geographical regions. Here, we explore the effect of cloudy and clear-sky conditions on the capability of ERA5 to correctly identify ice supersaturated regions, and the effect of varying the RHi threshold in ERA5. Again, we only consider the three atmospheric layers due to low sampling of the ~~number of ice particles~~ ice crystal number concentration in IAGOS, as described in Sect. 3.3.

~~Table 5 displays the ETS of cloudy, clear-sky and indeterminate conditions for the different geographic regions in the different atmospheric layers. Note that for this analysis we consider conditions with 250+ samples instead of 500+ samples, as done previously, due to less measurements with number of ice particles within IAGOS. However, as seen in Sect. S1 in the Supplement, 250+ samples should still be sufficient for the calculation of the ETS .~~

~~The main observation is that the ETS is highest in~~ Figure 12 and Fig. 13 display the ETS for clear-sky ~~conditions and lowest in cloudy and indeterminate conditions in the extratropics~~ and cloudy conditions for different ERA5 RHi thresholds. In clear-sky conditions, we find an ETS of approximately 0.15 in the extratropic UT and TP. This indicates a weak coherence in the prediction of ISSRs between IAGOS and ERA5 ~~.~~ and is the result of the clear-sky dry bias in ERA5 discussed in Sect. 3.3. The ETS reduces to between 0 and 0.05 in the clear-sky LS due to the rare occurrence of ISSRs and the underestimation of ISSRs by ERA5. For ~~indeterminate conditions, the ETS reduce to less than 0.1 in the UT and TP, except in North Asia, where it ranges between 0.11 and 0.14. For~~ cloudy conditions, the ETS is between 0.05 and 0.08 in most extratropic regions, indicating an almost purely random relationship between IAGOS and ERA5, which is most likely resulting from the saturation adjustment in the IFS. In North America, we find the ETS in the cloudy UT to be 0.14, showing a ~~more~~ weak coherence. No ETS are calculated in the extratropic TP or LS under cloudy conditions due to insufficient samples. ~~This means~~

In the tropics, the ETS is generally 0.05 in the clear-sky UT and show little increase or decrease in the TP when considering the RHi = 100% threshold. In the cloudy UT, the tropics shows an ETS of 0.1 or less, showing an almost entirely random relationship. The lower ETS in the tropics is also inline with the results presented in Sect. 3.4 and shows that ERA5 ~~shows better skill at predicting ISSR conditions~~ has little to no skill in predicting ISSR occurrence in tropic regions.

We find that by lowering the ERA5 RHi threshold, we can improve the predictive skills of ERA5 under clear-sky conditions~~, albeit it is a weak relationship.~~

~~The weak coherence in the extratropic UT~~ . In the extratropics, the threshold of 85% shows the best ETS in the UT and TROP, although we only achieve an increase in the ETS by approximately 0.1. In the extratropic LS, we generally need to decrease the threshold to 75% to achieve a better ETS, except in North Asia. The improved scores still indicate a weak relationship. In the tropical UT and TP, we also find that we can increase the ETS by 0.1 on average when reducing the ERA5 RHi threshold to the range of 75–85% under clear-sky conditions ~~is most likely the result of the clear-sky dry bias in ERA5, discussed in Sect. 3.3. Teoh et al. (2022) found~~ . In the tropopause in Africa, we find that the ETS ~~could be improved by lowering the RHi threshold for ISS, which we also discussed in Sect. 3.3, where the PDFs could be used to identify the necessary threshold~~ increases by 0.2 when lowering the ERA5 RHi threshold to ~~apply for each region. For cloudy and indeterminate conditions,~~ 75%.

Reducing the ERA5 RHi threshold under cloudy conditions in North America and North Asia also allows for minor improvements in the prediction of ISSRs in ERA5. In the North Atlantic and Europe, the ~~almost random relationship may be the result of the saturation adjustment in the IFS, given that we are matching the clear-sky, cloudy~~ best threshold appears to be 99%, without showing much improvement in the ETS. In the North Atlantic, the hit rate and false alarm are both high at the threshold of 100%. As the RHi threshold is decreased, both the hit rate and false alarm increase such that they are almost equal, while lowering the ETS. We see a similar occurrence in Europe; the difference is that the false alarm rates are lower, resulting in an ETS that is higher than in the North Atlantic. While this also occurs in North America and North Asia, the increase in the false alarm rate with the decrease in RHi threshold is not as high as in the North Atlantic or in Europe. The same reasoning also applies to the tropical regions. Hence, while lowering the RHi threshold does increase the number of correctly predicted ISSRs in ERA5, it comes at the cost of more false positives.

~~**Table 5.** Equitable threat score from prediction of ISSRs under clear-sky, cloudy and indeterminate conditions in ERA5 in upper troposphere (UT), tropopause (TP) and the lower stratosphere (LS). The different conditions have been matched between IAGOS and ERA5. Only combinations with 250+ samples are considered.~~

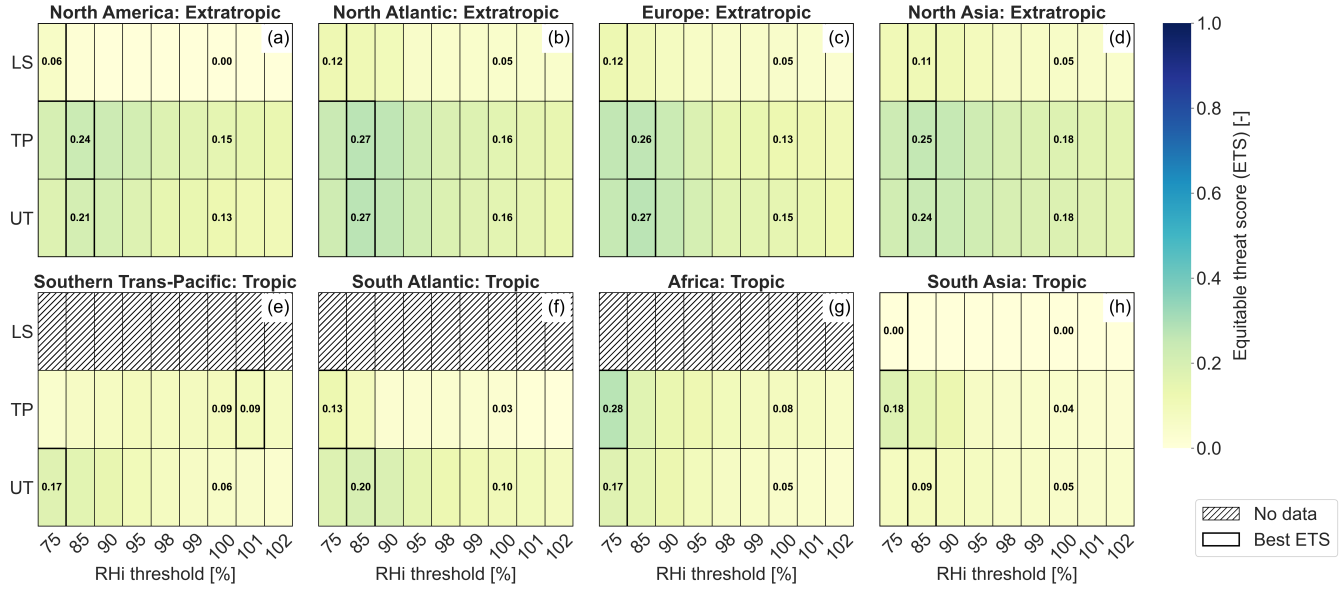

Figure 12. **(a–h)** Ice supersaturated region equitable threat score under clear-sky conditions for different ERA5 RHi thresholds in the upper troposphere (UT), tropopause (TP) and the lower stratosphere (LS). The different conditions have been matched between IAGOS and ERA5. Only combinations with 250+ samples are considered. For each layer, we highlight the ETS for a threshold of 100% and the ETS for the threshold at which we find the maximum value.

4 Discussion

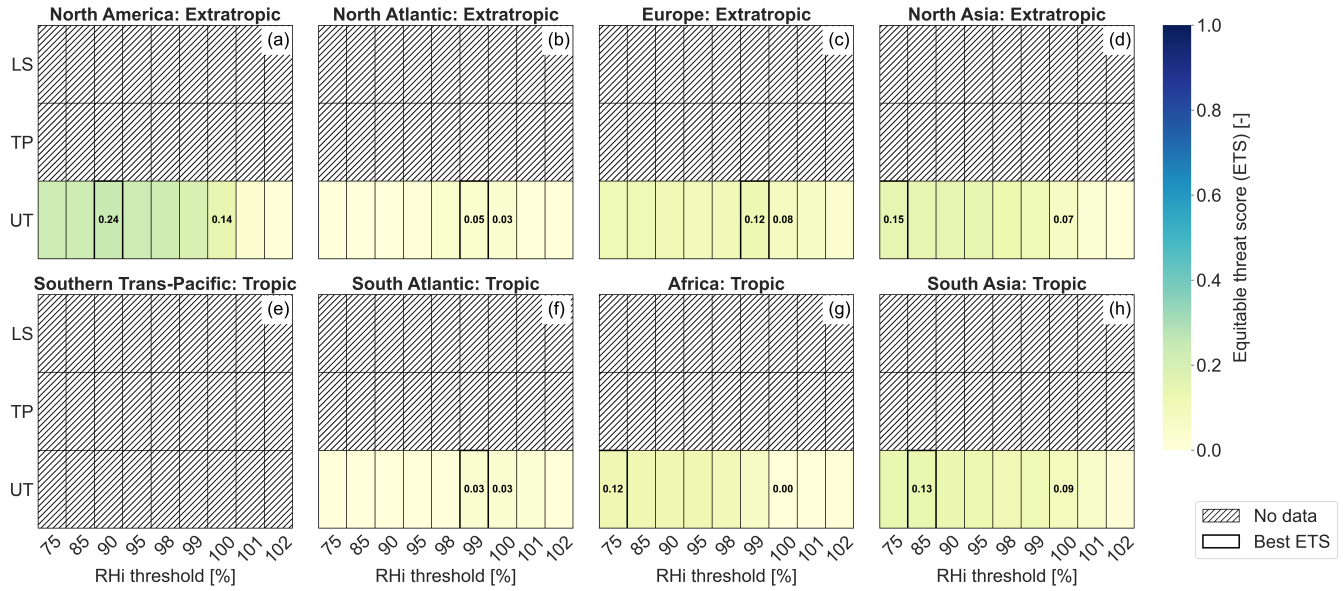

Figure 13. **(a–h)** Ice supersaturated region equitable threat score under cloudy conditions for different ERA5 RHi thresholds in the upper troposphere (UT), tropopause (TP) and the lower stratosphere (LS). The different conditions have been matched between IAGOS and ERA5. Only combinations with 250+ samples are considered. For each layer, we highlight the ETS for a threshold of 100% and the ETS for the threshold at which we find the maximum value.

The results presented in this paper largely agree with other studies. The extratropical cold bias of 0.5 K in ERA5 compared to IAGOS is in line with Wolf et al. (2025), who compared ERA5 and IAGOS in the mid-latitudes at different pressure levels. The observed extratropical lower stratospheric cold bias in ERA5 aligns with results from Shepherd et al. (2018), who reported a cold bias of up to 0.5 K in comparison to radiosondes in the lower stratosphere of ERA5 due to an underlying cold bias in the IFS. The vertical distribution of RHi using IAGOS measurements in the extratropics is similar to that reported by Petzold et al. (2020). The ERA5 extratropical dry bias is in line with other studies (Reutter et al., 2020; Wolf et al., 2025). We also observed a lower RHi from ERA5 than IAGOS in the lower stratosphere, but we cannot ascertain that it is due to biases in ERA5. In fact, some studies have also reported a general moist bias in the lower stratosphere in the ECMWF-IFS (Dyroff et al., 2014; Shepherd et al., 2018; Bland et al., 2021).

The overall behaviour of the RHi PDF under cloudy, clear-sky and indeterminate conditions in the UT and TROP is similar to that found by Wolf et al. (2025), but we find larger difference in the peak probability between IAGOS and ERA5 for cloudy and indeterminate conditions. If we consider the same geographic area, pressure levels and time frame for IAGOS measurements as Wolf et al. (2025) and do not consider separate atmospheric layers and do not normalise given the number of observations, we obtain more similar results to Wolf et al. (2025). We also found a low probability of RHi > 100% in the lower stratosphere using IAGOS measurements, which was also reported by Gierens et al. (1999) using the global distribution of MOZAIC flights and by Sanogo et al. (2024) in high-latitude regions (60–80° N) using IAGOS measurements. In South Asia, we also found that the

wet mode was subsaturated using IAGOS measurements. Sanogo et al. (2024) found similar observations when considering a larger tropical region. ~~This means that ERA5 cannot accurately predict the value of RHi within a cirrus cloud and may underestimate or overestimate ISSRs as a result.~~

In ~~the tropics, the ETS is generally 0.05 in the clear-sky UT and show little increase or decrease in the TP. The ETS is 0 in the LS due to no ISSRs. In the cloudy and indeterminate UT, the tropics shows an ETS of 0.1 or less, showing an almost entirely random relationship. The lower ETS in the tropics is also inline with the results presented~~ terms of the ISSR fraction, we observed that the ISSR fraction in the tropics increased up to just below the tropopause, and reached a maximum of 20% when looking at IAGOS. This is similar to Sanogo et al. (2024), who reported a maximum ISSR fraction of 15% in the tropics using IAGOS; the ISSR frequency varied about 5% or less among the four considered seasons in the tropics. Lamquin et al. (2012) also observed increasing ISSR occurrence with altitude in the tropics using MOZAIC, with maximum ISSR frequencies of up to 30%, but this study considered the frequency per individual grid box. The vertical structure of the ISSR fraction found using IAGOS measurements in the extratropics is also consistent with earlier findings (Petzold et al., 2020; Reutter et al., 2020; Sanogo et al., 2024), but we observe some variance in the maximum ISSR fraction reported with IAGOS/MOZAIC. A maximum ISSR fraction of 40% was found when considering all seasons (Reutter et al., 2020) and 20% in the midlatitudes for DJF and MAM (Sanogo et al., 2024). However,the ISSR fraction is sensitive to the number of samples and these studies use different subsets of the IAGOS/MOZAIC dataset.

We also found that the ISSR fraction is generally underestimated by ERA5 due to the observed dry bias. Reutter et al. (2020) observed the same for ERA-interim when considering the North Atlantic region. In instances where the RHi is overestimated by ERA5, such as in South Asia for season JJA, the ISSR fraction is overestimated by ERA5. Agarwal et al. (2022) found a tendency for ERA5 to overestimate the ISSR occurrence at cruise altitudes in the tropics and mid-latitudes when compared to radiosonde measurements. However, the radiosonde measurements are not corrected for dry biases and the location of these radiosonde observations are generally over land and not very widespread as with the IAGOS measurements, which could lead to differences in obtained results.

Gierens et al. (2020a) calculated ETS between 0.05 and 0.25, depending on the season. The value of 0.05 is on the lower side compared to the results in Sect. 3.4, but this may be because the study does not take into account the different atmospheric layers or regions, and it also only considers four months of IAGOS measurements. If we do not take into account the vertical layers defined, the ETS remains between 0.15 and ~~shows that~~ 0.3. Hence, the low ETS found by Gierens et al. (2020a) is most likely the result of using a smaller subset of IAGOS and ERA5 ~~has little to no skill in predicting ISSR occurrence in tropic regions~~data. The study by Wang et al. (2025) shows an ETS of 0.23 upper troposphere (UT) and 0.14 in the lower stratosphere before application of the machine learning algorithm, which agrees well with the values identified in this study.

~~Wang et al. (2025)~~We find different ETS scores in clear-sky and cloudy conditions compared to Wang et al. (2025), who found an ETS score of 0.06 in clear-sky upper troposphere and lower stratosphere (UTLS). In the cloudy UTLS, Wang et al. (2025) calculated an ETS score of 0.23. These different ETS scores are ~~most likely~~ the result of using different methodologies for classifying cloudy and clear-sky conditions. Wang et al. (2025) uses the specific cloud ice water content from ERA5 to determine if a point is within a cloud or in clear-sky. Other papers use the ~~number of ice particles~~ ice crystal number

concentration to determine cloudy conditions in IAGOS measurements (Petzold et al., 2017; Sanogo et al., 2024; Wolf et al., 2025), but the reporting of cloudy conditions compared to ERA5 appears relatively new. Only Wolf et al. (2025) and Wang et al. (2025) seem to have considered such a comparison, but use different variables to determine ~~cloudiness~~ in-cloud conditions in ERA5. ~~Hence, it raises the question for the correct procedure for classifying a point as cloudy or clear-sky.~~

4.1 ~~Prediction of ice supersaturated regions in ERA5 for different North Atlantic weather patterns~~

~~As discussed by Irvine et al. (2012), there is a dependency of ice supersaturated region occurrence on different North Atlantic weather patterns. In this section, we explore if they also have an impact on the biases to expect in~~ As discussed in Sect. S1 in the supplement, the cloud ice water content definition is limited in identifying clear-sky ice supersaturated conditions. In contrast, the ice crystal number concentration in IAGOS and the cloud cover definition in ERA5 ~~. We consider eastbound and westbound routes separately as eastbound routes tend to take advantage of the jet stream to reduce fuel consumption.~~

~~Figure 14 shows the ETS for the winter and summer weather patterns on the eastbound routes. The summer weather patterns appear to have no effect on the ETS, however, these patterns are also weaker than the winter weather patterns due to weaker teleconnection patterns and less variation of the jet stream latitude (Irvine et al., 2013). For the winter weather patterns, we find a tendency for W1, W2 and W4 to have a lower ETS compared to W3 and W5, except at 60 hPa below the tropopause and in the lower stratosphere. In the lower stratosphere, all winter weather patterns have almost equal ETS, except for W2, which has a higher ETS. Irvine et al. (2012) found that W2 showed a higher frequency of ISSRs at higher altitudes when using ERA-Interim. We find that~~ are more suitable for analysing ice supersaturation in clear-sky and cloudy conditions. Hence, we recommend using the latter definition.

In an attempt to identify when biases in ERA5 ~~shows a slightly higher ISSR fraction in the lower stratosphere compared to IAGOS, but the difference is less than 1% and can therefore not be considered significant. Hence, the larger ETS for W2 in the lower stratosphere most likely arises from low ISSR occurrence in combination with the slightly higher ISSR fraction in~~ might arise and how to correct them, we recommend as future research to explore the correlation between weather pattern and the ability of ERA5 ~~. Between 30 hPa from the tropopause and the tropopause itself, W1, W2 and W4 have an ETS between 0.15 and 0.2, showing a weak coherence between IAGOS and~~ to estimate ISSRs. As an example, we explored whether the type of North Atlantic weather pattern can affect the observed biases in ERA5 ~~in the prediction of ISSRs. For W3 and W5,~~ since Irvine et al. (2012) found that the ~~ETS improves to the range 0.2 to 0.25, but this is still a weak to mediocre coherence. The main difference between these two groups of weather patterns is their jet stream strength. That is, W1, W2 and W4 are classified as having a strong jet stream and W3 and W5 have a weak jet stream.~~

~~The question that arises is how the characteristics of the different weather patterns affect ISSR occurrence. For example, Irvine et al. (2012) showed that for W4, the ridge over the Atlantic is most pronounced, which leads to high frequency of ISSRs over Greenland and low ISSR occurrence south of the jet stream,~~ probability of forming contrails as a function of altitude depends on the weather patterns when using ERA-Interim. ~~Eastbound flights fly at these more southern latitudes (Irvine et al., 2012). Due to ISSRs being a more rare occurrence along eastbound routes for W4, also seen in the IAGOS ISSR fraction, it could lead to ERA5 predicting less of the ISSRs that do occur. We also find a lower ISSR fractions for W1 and~~

W2 using IAGOS. Hence, we see a tendency for lower ISSR occurrence in IAGOS leading to a lower ETS, indicating a lower predictive skill for ERA5. Whether the jet stream strength or jet stream position are the reason for the changes in the ISSR occurrence and how it can impact the ability The methodology is explained in the supplement (Sect. S7). The variability of ERA5 to predict ISSRs requires further research. Irvine et al. (2012) did find changes in the ISSR frequency between biases under the five winter weather patterns , but this study only considered ERA-Interim, which is also known to have issues in the prediction of ISSRs (Reutter et al., 2020).

Figure 14. Vertical distribution of ETS from prediction of ISSRs in ERA5 on eastbound routes over the North Atlantic for **a)** winter and **b)** summer weather patterns. Only combinations of weather pattern and vertical level with 250+ samples are considered.

Figure 15 shows the vertical distribution of the ETS on westbound routes for the winter and was found to be larger than the one under the three summer weather patterns. Again, no significant differences are found between the summer weather patterns, which are weaker. For the winter weather patterns, we do not find large differences in the ETS, except near or at the tropopause, or at a distance of 100 hPa or more below the tropopause. Irvine et al. (2012) also found smaller differences in the probability of forming contrails between each winter weather type for westbound time-optimal routes, which were also lower than eastbound time-optimal routes. We also generally find lower ISSR fractions for each winter weather type on westbound routes compared to eastbound routes , except for W4. This could be related to the higher ISSR occurrence at more northern latitudes compared to southern latitudes for W4 (Irvine et al., 2012), where we also find the mean latitude of westbound IAGOS flights to be more north compared to eastern bound flights.

While the ISSR fraction tends to be lower for western bound flights, the ETS is shifted to slightly higher values. This shows a somewhat better agreement between IAGOS and ERA5 see more distinct weather dependency of the biases on eastbound routes compared to on westbound routes. We theorise that it could be related to the distribution of ISSRs that result from each winter weather pattern type. For example, suggest that this could be due to the variability of the jet stream location and strength, which determines the distribution of ISSRsmay be more patchy close to and along the jet stream, but larger ISSRs are found further from the jet stream, which ERA5 may be better able to predict. In fact, Irvine et al. (2012) showed different distributions and frequencies of ISSRs in ERA-Interim for the different winter weather patterns, where a less patchy area of high ISSR frequency was found over Greenland compared to along the jet stream. However, this was averaged over several winters and thus, we cannot identify if the larger areas are due to averaging or if there exists larger areas of ISSRs at more northern latitudes. To understand if the distribution of ISSRs under different winter weather patterns impact the ability of , although the interpretation of these findings requires further investigation.

Another factor influencing our conclusions is the availability of IAGOS measurements. Without enough measurements, our conclusions may not be representative. Therefore, we evaluated the necessary number of points needed to be confident in our results (see Sect. S2 in the supplement). Nevertheless, there are still some limitations. In our evaluation on the prediction of ISSRs in ERA5 to predict ISSRs, it would be necessary to analyse the daily variability of ISSRs as the jet stream position and strength can show variation within the weather pattern itselfunder cloudy and clear-sky conditions, we lowered the minimum sample size required for a representative result due to low sampling of the ice crystal number concentration in IAGOS. This

results in a larger variability of the ETS, and thus the true value may be higher or lower than reported, though, the 95% confidence interval lies close to the mean of 100 tests. Nevertheless, for future work, we recommended to increase the number of IAGOS aircraft capable of measuring the ice crystal number concentration to further distinguish between cloudy and clear-sky conditions.

Figure 15. Vertical distribution of ETS from prediction of ISSRs in ERA5 on westbound routes over the North Atlantic for **a)** winter and **b)** summer weather patterns. Only combinations of weather pattern and vertical level with 250+ samples are considered.

5 Conclusions

In this study, we evaluated ERA5 temperature, relative humidity over ice (RHi) and ice supersaturated region (ISSR) occurrence against IAGOS in situ measurements over the period 2011-2022. 2011–2022. Differences in the frequency of ice supersaturation (ISS) were also compared. The analysis was performed over a large geographical area covering the tropics and extratropics. It included the upper troposphere (UT) and lower stratosphere (LS), with vertical levels defined based on distance to the thermal tropopause. The RHi and ISSR occurrence is also documented for cloudy and clear-sky conditions. We used the number of ice particles ice crystal number concentration in the IAGOS measurements and the cloud cover in ERA5 to distinguish between cloudy, clear-sky and indeterminate conditions. The impact of different North Atlantic weather patterns on ERA5s ability changing the ERA5 RHi threshold on the ability of ERA5 to predict ISSRs was also investigated. The main conclusions of our study are as follows:

1. The vertical distribution of temperature and relative humidity over ice was analysed per season and region for IAGOS and ERA5. Temperature differences between IAGOS and ERA5 were mainly a function of the atmospheric layer, with a larger cold bias in the LS. ERA5 showed a dry bias in RHi for all atmospheric layers, but the lower stratospheric biases differences in the lower stratosphere may be due to limitations of the IAGOS ICH sensor. Larger dry biases were found in colder months in the extratropics due to larger values of RHi being possible occurring in these conditions. A moist bias was identified in South Asia for season JJA.

2. We characterised the PDF of RHi in the UT, the tropopause (TROP) and the LS for cloudy, clear-sky and indeterminate conditions. In clear-sky conditions, ERA5 showed an underestimation of ISS. In cloudy conditions, ERA5 displayed large peaks centred at RHi = 1RHi = 100%, due to the scheme that lowers RHI RHi to saturation when clouds are present (saturation adjustment). This is more critical in the UT and TROPas , since the LS is dry and cloud occurrence is rare, with little to no ISS conditions. While this generally also results in a dry bias, it can also cause a moist bias if the wet mode of the RHi PDF is subsaturated.

3. ERA5 shows showed a general underestimation of ISSRs in comparison to IAGOS due to biases in the RHi. The ability of ERA5 to predict ISSRs was estimated using the equitable threat score (ETS). It showed With an RHi threshold of 100%, ERA5 shows a weak to mediocre correlation between IAGOSand with IAGOS. We found that the ability of

ERA5 ~~in the prediction of ISSRs, with a weaker coherence in the tropics compared to the extratropics.~~ to predict ISSRs can be improved by decreasing the ERA5 ~~also showed a better ETS in fall and winter compared to summer and spring in the extratropics, but no seasonal dependence was identified in the tropics. The lowest ETS was found for South Asia in seasonJJA, which is most likely the result of ERA5 not being able to predict the subsaturated wet mode of the RHi PDF due to the saturation adjustment. For this region and season, the ISSR fraction was also overestimated by~~ RHi threshold. The optimal value ranges between 85% to 95% in the upper troposphere and tropopause, and it shows a dependency on the region, distance from the tropopause and the season, with more improvements possible in DJF compared to JJA. However, the improvement is limited, as ETS values do not exceed about 0.5 in DJF and 0.3 in JJA. In the lower stratosphere, RHi threshold adjustments have little effect on the predictive skills of ERA5~~in comparison to IAGOS~~.

4. The ETS for various ERA5 RHi thresholds was also calculated for the prediction of ISSRs under cloudy, clear-sky and indeterminate conditions. It showed a better coherence between IAGOS and ERA5 for clear-sky conditions compared to cloudy conditions, particularly in the extratropics. Better predictive skills of ERA5 can generally be achieved by lowering the RHi threshold to the range of 75% to 85%, albeit the improvements are limited and ERA5 still exhibits a weak to mediocre correlation with IAGOS. The ETS values for cloudy conditions indicate an almost random relationship~~, showing ERA5 cannot accurately predict ISSRs under such conditions. The tropics showed almost random relationships for both cloudy and clear-sky conditions.~~ . Improvements from lowering the RHi threshold are constrained by the resulting increase in false alarms.

5. ~~The influence of the North Atlantic weather patterns on ERA5s capability to predict ISSRs was also investigated using the ETS. The winter weather patterns resulted in stronger differences between each type of pattern compared to summer weather patterns. This is the result of weaker summer patterns. For the winter weather pattern, we see more distinct differences between each weather type on eastbound routes compared to on westbound routes. We theorise it could be due to the distribution of ISSRs due to the jet stream, but it requires further investigation.~~

This study is an extension of previous studies comparing IAGOS and ERA5, such as Gierens et al. (2020a) and Wolf et al. (2025). These studies also find ERA5 to underestimate ISSR occurrence compared to ~~in-situ~~ in situ measurements due to biases in estimation of RHi in ERA5. However, they are limited in their regional and seasonal coverage. Our analysis considers geographical areas not covered in the previously mentioned studies, such as the tropics, and provides a seasonal comparison within each subregion considered. It shows that we cannot assume that ERA5 has the same ability to predict ISSRs in different subregions and that ERA5 has less ability to predict ISSRs in the tropics. Our seasonal comparison reveals a similar seasonal pattern in ISSR occurrence in the extratropics as reported in previous studies, but we further find that the ability of ERA5 to predict ISSRs can itself be seasonally dependent.

With regard to the comparison of ice supersaturation in cloudy, clear-sky and indeterminate conditions, we find comparable results in the RHi PDF in the extratropics to those of Wolf et al. (2025), and the IAGOS RHi PDF closely resembled the results obtained by previous studies. We find larger differences in the peak probability of RHi between IAGOS and ERA5 under cloudy and indeterminate compared to Wolf et al. (2025), most likely due to the consideration of the atmospheric layers

in this study. Moreover, we extended the analysis to the tropics and also quantified how cloudy, clear-sky and indeterminate conditions affect the ability of ERA5 to predict ISSRs, which was shown to be driven by the clear-sky dry bias in RHi and the saturation adjustment in ERA5. Wang et al. (2025) calculated the ETS for RHi > 100% with IAGOS and ERA5 under cloudy and clear-sky conditions, for which a higher ETS was found for cloudy conditions compared to clear-sky for a a dataset covering the upper troposphere and lower stratosphere. Wang et al. (2025) used a different methodology to detect clear-sky and cloudy conditions compared to this study. ~~Thus, we recommend to adapt a standard methodology for comparing IAGOS~~ We recommend to use the ice crystal number concentration from IAGOS and the cloud cover from ERA5 for comparing ISSRs under cloudy and clear-sky conditions ~~to cloudy and~~ between the two datasets due to the limitations of the cloud ice water content under clear-sky conditions~~in ERA5~~.

The ~~analysis is highly dependent on the number of available measurements from IAGOS and without enough measurements, our conclusions may not be representative. While we did evaluate the necessary number of points needed to be confident in our results and presented results with respect to these findings, there are still some limitations. In our evaluation on the prediction of ISSRs in ERA5 under cloudy and clear-sky conditions, we lowered the~~ representativeness of our results was also influenced by the availability of IAGOS measurements, particularly the sampling of the ice crystal number concentration. While the minimum sample size required for ~~a representative result~~ statistical robustness was evaluated, we had to relax this threshold for some analyses due to low sampling~~of the number of ice particles in IAGOS. This results in~~ , resulting in a larger variability of the ETS~~, and thus the true value may be higher or lower than reported, though, the 95% confidence interval lies close to the mean of 100 tests. Nevertheless, for future work, we recommended to increase~~ . For example, this was done in the analyses on the prediction of ISSRs under cloudy and clear-sky conditions. Increasing the number of IAGOS aircraft capable of measuring the ~~number of ice particles to further distinguish between~~ ice crystal number concentration would enable clearer separation of cloudy and clear-sky conditions~~. For the North Atlantic weather pattern analysis, we also lowered the minimum sample size to better evaluate differences in the vertical distribution, which may have similar implications. Thus, we recommend to expand the analysis with more measurements in the future, if and when available. While the evaluation of the North Atlantic weather patterns on the ability of ERA5 to predict ISSRs indicated a possible dependence on winter weather patterns, the underlying cause remains uncertain. Hence, the effect of jet stream strength and position on ISSR occurrence and how it impacts the ability of ERA5 to predict ISSRs should be further researched and quantified before making definitive conclusions~~, while improving the assessment of RHi and ISSRs under such conditions.

Based on the results of this study, the lack of ISS in clear-sky conditions is a key limitation in the ERA5 reanalysis dataset and should be addressed. Otherwise, ISSRs are systematically underestimated, potentially leading to an underestimation of the occurrence of persistent contrails and, consequently, uncertainties in their estimated climate impact. The lack of ISS may ~~temporarily~~ for the time being be improved by decreasing the RHi threshold for ISS, ~~but~~ although this is only applicable to regions where ~~we have in-situ measurements , limiting their global applicability~~in situ measurements are available. The analysis also shows that the application of the saturation adjustment in the NWP model underlying the reanalysis should be revisited to properly account for ISS under cloudy conditions~~as it~~ , as the current approach contributes to inaccuracies in the prediction of ISSRs in ERA5. ~~The influence of the jet stream strength and position on the distribution of ISSRs and the ability of ERA5~~

~~to predict ISSRs may also provide further insight into how ISSRs, and thus persistent contrails, could be avoided based on the weather pattern.~~ Overall, these findings improve our understanding regarding the variability of ISSRs and the extent to which ERA5 is able to accurately predict ~~ISSRs~~ them under different conditions. This has important implications for the accurate assessment of aviation induced persistent contrail formation, which can have a significant effect on the local radiative budget.

Code and data availability. The Python code used to perform the analysis in this study is publicly available via the following DOI: 10.4121/915dc859-c397-4294-8e85-83451ebaa881.

The IAGOS data can be obtained from the IAGOS data portal at https://doi.org/10.25326/20. The Analysis-Ready, Cloud Optimized (ARCO) ERA5 data can be obtained from Google Cloud Storage at https://console.cloud.google.com/marketplace/product/bigquery-public-data/arco-era5. The ERA5 data can be obtained from the ECMWF data catalog at https://doi.org/10.24381/cds.f17050d7 (Hersbach et al., 2023b). The ERA5 reanalysis tropopause data can be found here: https://datapub.fz-juelich.de/slcs/tropopause/

Appendix A: Distribution of temperature and relative humidity over ice ~~with respect to thermal and dynamic tropopause~~in the Southern Hemisphere Tropics

We have analysed the impact of considering different latitudinal bands in the defined tropical regions, where we considered the bands 0 to 30° N and 0 to 30° S, while keeping the same longitudinal bands. Figure A1 shows the results for the Southern Hemisphere (the Northern Hemisphere results are found in Fig. 6).

We find that there is a reversal of the seasonal behaviour of RHi between these two latitudinal bands in South Asia. When considering the latitudinal band 0 to 30° N, the highest RHi values throughout the vertical profile occur during season JJA and the lowest in DJF. However, in the latitudinal band of 0 to 30° S, the highest RHi values occur in DJF and the lowest in JJA. This could be the due to the seasonality of the location of the inter-tropical convergence zone (ITCZ), which can result in opposite behaviour across the equator (National Oceanic and Atmospheric Administration, 2023). For example, we could find dry conditions in the Northern Hemisphere and wet conditions in the Southern Hemisphere in the same region (National Oceanic and Atmospheric Administration, 2023). In the South Atlantic and in Africa, we find a more distinct seasonal variation of the vertical distribution of RHi in the latitudinal band of 0 to 30° S compared to the band of 0 to 30° N. We do not find any measurements in the Southern Trans-Pacific between 0 to 30° S. To conclude, when considering the seasonality in the tropics, we recommend to consider to Northern and Southern Hemisphere separately.

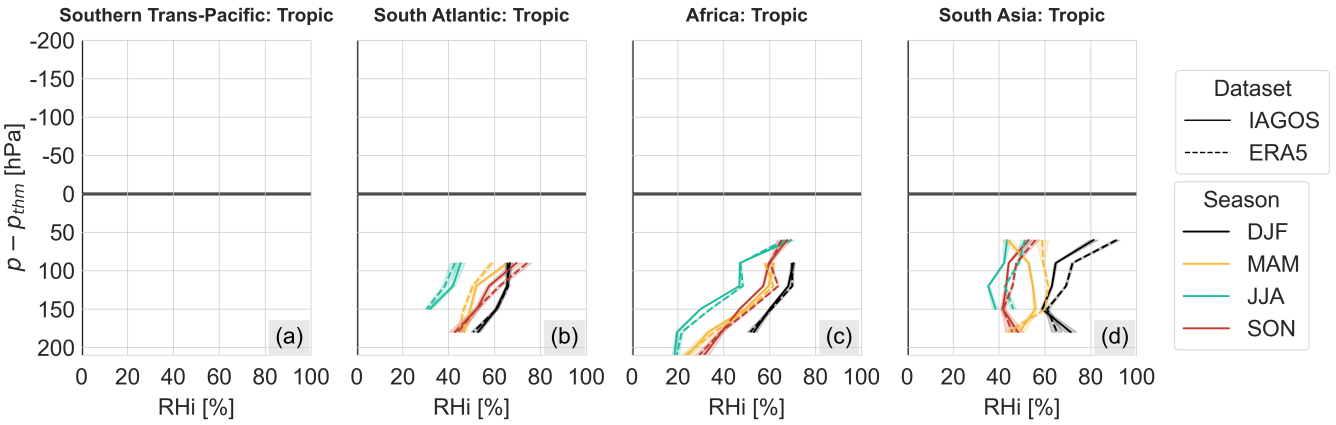

Figure A1. (a–d) Vertical distribution of IAGOS and ERA5 mean relative humidity over ice per season in the Southern Hemisphere tropical regions, with shading showing the 95% confidence interval. Vertical levels are shown in terms of distance to the thermal tropopause ($p - p_{thm}$). We only consider vertical levels, seasons and regions with 500+ samples.

Appendix B: Distribution of temperature and relative humidity over ice with respect to thermal and dynamic tropopause

In this appendix, we present the vertical distribution of temperature and relative humidity over ice with respect to the thermal and dynamic tropopause. The tropopause data for both definitions are extracted from Hoffmann and Spang (2022). Since there can be two thermal tropopauses according to the World Meteorological Organization (WMO) definition (Hoffmann and Spang, 2022), we only consider the first ~~thermal tropopausefound~~WMO tropopause.

Figure B1 shows the vertical distribution of temperature and relative humidity over ice for the thermal and dynamic tropopause definitions ~~.~~ from 1 July 2011 to 31 December 2022. We find similar distributions with both definitions, ~~though~~ although there are some differences. For the vertical distribution of temperature, the dynamical and thermal tropopause ~~shows~~ show similar values for the mean and the 25% and 75% percentiles, especially in the upper troposphere. In the lower stratosphere, it is noticeable that the temperature gradient is sharper across the thermal tropopause in comparison to the dynamic tropopause. For the 99% percentile, we notice that the thermal tropopause also has a sharper gradient in the upper troposphere, ~~but~~ while for the 1% percentile it is stronger for the dynamic tropopause. This is similar to observations by Petzold et al. (2020).

Larger differences between the two tropopause definitions are noticeable for the vertical distribution of relative humidity over ice. In the lower stratosphere, larger values of RHi are found when using the dynamic tropopause definition, due to the larger 99% percentile range, for which the thermal tropopause definition shows a sharper vertical gradient. This is also shown by the smaller mean RHi for the thermal tropopause compared to the dynamic tropopause. This may be the result of the thermal tropopause being located at a higher altitude than the dynamical tropopause (Petzold et al., 2020), for which drier conditions may be observed with this definition. This is also inline with reports by Petzold et al. (2020), who found a lower ISSR fraction in the lower stratosphere when using the thermal tropopause definition compared to the dynamic tropopause,

indicating more moist conditions with the latter definition. We also find that the thermal tropopause is drier in the upper troposphere in comparison to the dynamic tropopause.

This analysis shows that the results are impacted by the choice of the tropopause definition. However, in this study, we are interested in the differences ~~that exist~~ between IAGOS and ERA5~~. Hence, due to~~ , and are interested in the separation of dry and moist conditions. Although there are no significant differences in the results when using the thermal and dynamic tropopause definitions, there is a tendency for the dynamic tropopause definition to result in higher values of RHi in the lower stratosphere compared to the ~~sharper gradients for the~~ thermal tropopause ~~, we will use this definition for the study~~definition. Therefore, we decided to use the thermal tropopause to ensure better separation of moist and dry conditions.

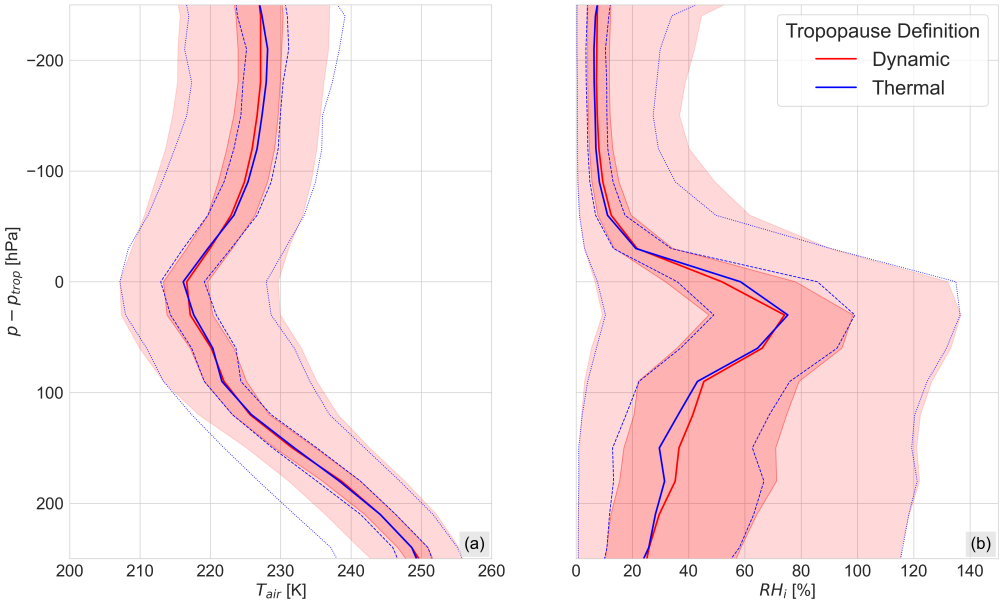

Figure B1. Vertical distribution of **a)** temperature and **b)** RHi for dynamic and thermal tropopause definitions using all considered IAGOS measurements in this study. Solid ~~line indicates the~~ lines indicate mean ~~,~~ values; dashed ~~(~~blue ~~)~~ line and dark ~~(~~red ~~)~~ shade indicate the 25 and 75% percentiles ~~,~~ at the thermal and dynamical tropopause, respectively; similarly, dotted ~~(~~blue ~~)~~ line and light ~~(~~red ~~)~~ shade indicate the 1 and 99% percentiles.

Author contributions. KGH and FY designed the study. KGH performed the data analysis and prepared the manuscript under the supervision of FY. FC applied the North Atlantic weather pattern classification. FC, VM, FY and KGH reviewed and edited the manuscript.

Competing interests. The contact author has declared that none of the authors has any competing interests.

Acknowledgements. We acknowledge the strong support of the European Commission, Airbus, national agencies in Germany (BMBF), France (MESR), and the UK (NERC), and the IAGOS member institutions (http://www.iagos.org/partners), and the airlines (Lufthansa, Air France, Austrian, China Airlines, Hawaiian Airlines, Air Canada, Iberia, Eurowings Discover, Cathay Pacific, Air Namibia, Sabena) that have carried the MOZAIC or IAGOS measurement equipment free of charge and performed maintenance since 1994. The data are available at http://www.iagos.fr thanks to additional support from AERIS. IAGOS has been funded by the European Union projects IAGOS–DS and IAGOS–ERI, INSU-CNRS (France), Météo-France, Université Paul Sabatier (Toulouse, France), and Forschungszentrum Jülich (FZJ, Jülich, Germany).

Financial support. This research has received funding from the Horizon Europe Research and Innovation Actions programme under Grant Agreement No 101056885 and from Horizon Europe Research and Innovation Actions programme under Grant Agreement No 101167020.

References

Agarwal, A., Meijer, V., Eastham, S. D., Speth, R. L., and Barret, S. R. H.: Reanalysis-driven simulations may overestimate persistent contrail formation by 100%–250%, Environmental Research Letters, 17, https://doi.org/10.1088/1748-9326/ac38d9, 2022.

Alduchov, O. A. and Eskridge, R. E.: Improved Magnus Form Approximation of Saturation Vapor Pressure, Journal of Applied Meteorology and Climatology, 35, 601 – 609, https://doi.org/10.1175/1520-0450(1996)035<0601:IMFAOS>2.0.CO;2, 1996.

Arriolabengoa, S., Crispel, P., Jaron, O., Bouteloup, Y., Vié, B., Li, Y., Petzold, A., and Plu, M.: Modeling and verifying ice supersaturated regions in the ARPEGE model for persistent contrail forecast, Atmospheric Chemistry and Physics, 25, 18 051–18 076, https://doi.org/10.5194/acp-25-18051-2025, 2025.

Avila, D., Sherry, L., and Thompson, T.: Reducing global warming by airline contrail avoidance: A case study of annual benefits for the contiguous United States, Transportation Research Interdisciplinary Perspectives, 2, 100 033, https://doi.org/10.1016/j.trip.2019.100033, 2019.

Bland, J., Gray, S., Methven, J., and Forbes, R.: Characterising Extratropical Near-Tropopause Analysis Humidity Biases and Their Radiative Effects on Temperature Forecasts, Quarterly Journal of the Royal Meteorological Society, 147, https://doi.org/https://doi.org/10.1002/qj.4150, 2021.

Carver, R. and Merose, A.: ARCO-ERA5: An Analysis-Ready Cloud-Optimized Reanalysis Dataset, 22nd Conf. on AI for Env. Science, Denver, CO, Amer. Meteo. Soc, 4A.1,, https://ams.confex.com/ams/103ANNUAL/meetingapp.cgi/Paper/415842, 2023.

Delft High Performance Computing Centre: DelftBlue Supercomputer (Phase 2), https://www.tudelft.nl/dhpc/ark:/44463/DelftBluePhase2, (last access: 2025-04-30), 2024.

Driver, O. G. A., Stettler, M. E. J., and Gryspeerdt, E.: The ice supersaturation biases limiting contrail modelling are structured around extratropical depressions, Atmospheric Chemistry and Physics, 25, 16 411–16 433, https://doi.org/10.5194/acp-25-16411-2025, 2025.

Dyroff, C., Zahn, A., Christner, E., Forbes, R., Tompkins, A., and van Velthoven, P.: Comparison of ECMWF analysis and forecast humidity data with CARIBIC upper troposphere and lower stratosphere observations, Quarterly Journal of the Royal Meteorological Society, 141, https://doi.org/10.1002/qj.2400, 2014.

ECMWF: L137 model level definitions, https://confluence.ecmwf.int/display/UDOC/L137+model+level+definitions, last access: 2025-05-07.

European Centre for Medium-Range Weather Forecasts (ECMWF): IFS Documentation – Cy41r2. Part IV: Physical Processes, Tech. rep., European Centre for Medium-Range Weather Forecasts, operational implementation: 8 March 2016, 2016.

Filippone, A.: Assessment of Aircraft Contrail Avoidance Strategies, Journal of Aircraft, 52, 872–877, https://doi.org/10.2514/1.C033176, 2015.

Gierens, K., Schumann, U., Helten, M., Smit, H., and Marenco, A.: A distribution law for relative humidity in the upper troposphere and lower stratosphere derived from three years of MOZAIC measurements, Annales Geophysicae, 17, 1218–1226, https://doi.org/10.1007/s00585-999-1218-7, 1999.

Gierens, K., Spichtinger, P., and Schumann, U.: Ice Supersaturation, in: Atmospheric Physics: Background - Methods - Trends, Springer, https://doi.org/10.1007/978-3-642-30183-4_9, 2012.

Gierens, K., Matthes, S., and Rohs, S.: How Well Can Persistent Contrails Be Predicted?, Aerosapce, 7, https://doi.org/10.3390/aerospace7120169, 2020a.

Gierens, K., Wilhelm, L., Sommer, M., and Weaber, D.: On ice supersaturation over the Arctic, Meteorologische Zeitschrift, 29, https://doi.org/10.1127/metz/2020/1012, 2020b.

Hanst, M., Köhler, C. G., Seifert, A., and Schlemmer, L.: Predicting ice supersaturation for contrail avoidance: ensemble forecasting using ICON with two-moment ice microphysics, Atmospheric Chemistry and Physics, 25, 17 253–17 274, https://doi.org/10.5194/acp-25-17253-2025, 2025.

Hersbach, H., Bell, B., Berrisford, P., Hirahara, S., Horányi, A., Muñoz-Sabater, J., Julien Nicolas, C. P., Radu, R., Schepers, D., Simmons, A., Soci, C., Abdalla, S., Abellan, X., Balsamo, G., Bechtold, P., Biavati, G., Bidlot, J., Bonavita, M., Chiara, G. D., Dahlgren, P., Dee, D., Diamantakis, M., Dragani, R., Flemming, J., Forbes, R., Fuentes, M., Geer, A., Haimberger, L., Healy, S., Hogan, R. J., Hólm, E., Janisková, M., Keeley, S., Laloyaux, P., Lopez, P., Lupu, C., Radnoti, G., de Rosnay, P., Rozum, I., Vamborg, F., Villaume, S., and Thépaut, J.-N.: The ERA5 global reanalysis, Quarterly Journal of the Royal Meteorological Society, 146, https://doi.org/10.1002/qj.3803, 2020.

Hersbach, H., Bell, B., Berrisford, P., Biavati, G., Horányi, A., Muñoz Sabater, J., Nicolas, J., Peubey, C., Radu, R., Rozum, I., Schepers, D., Simmons, A., Soci, C., Dee, D., and Thépaut, J.-N.: ERA5 hourly data on pressure levels from 1940 to present. Copernicus Climate Change Service (C3S) Climate Data Store (CDS), https://doi.org/10.24381/cds.bd0915c6, (last access: 2025-05-14), 2023a.

Hersbach, H., Bell, B., Berrisford, P., Horányi, A., Sabater, J. M., Nicolas, J., Peubey, C., Radu, R., Rozum, I., Schepers, D., Simmons, A., Soci, C., Dee, D., and Thépaut, J.-N.: ERA5 monthly averaged data on single levels from 1940 to present. Copernicus Climate Change Service (C3S) Climate Data Store (CDS), https://doi.org/10.24381/cds.f17050d7, (last access: 2024-12-10), 2023b.

Hoffmann, L. and Spang, R.: An assessment of tropopause characteristics of the ERA5 and ERA-Interim meteorological reanalyses, Atmospheric Chemistry and Physics, 22, 4019–4046, https://doi.org/10.5194/acp-22-4019-2022, 2022.

IAGOS: Observed and Modelled Variables, https://iagos.aeris-data.fr/parameters/, last access: 2025-04-15a.

IAGOS: HUMIDITY SENSOR (ICH, PART OF PACKAGE1), https://www.iagos.org/iagos-core-instruments/h2o/, last access: 2025-04-15b.

IAGOS: IAGOS-CORE, https://www.iagos.org/iagos-core-instruments/, last access: 2025-04-15c.

IAGOS: IAGOS FLEET, https://www.iagos.org/iagos-fleet/, last access: 2025-04-15d.

IAGOS: DATA QUALITY, https://iagos.aeris-data.fr/data-quality/, last access: 2025-06-10.

Irvine, E. A., Hoskins, B. J., and Shine, K. P.: The dependence of contrail formation on the weather pattern and altitude in the North Atlantic, Geophysical Research Letters, 39, https://doi.org/10.1029/2012GL051909, 2012.

Irvine, E. A., Hoskins, B. J., Shine, K. P., Lunnona, R. W., and Froemming, C.: Characterizing North Atlantic weather patterns for climate-optimal aircraft routing, Meteorological Applications, 20, https://doi.org/10.1002/met.1291, 2013.

Konjari, P., Rolf, C., Hegglin, M. I., Rohs, S., Li, Y., Zahn, A., Bönisch, H., Nedelec, P., Krämer, M., and Petzold, A.: Technical note: Water vapour climatologies in the extra-tropical upper troposphere and lower stratosphere derived from a synthesis of passenger and research aircraft measurements, Atmospheric Chemistry and Physics, 25, 4269–4289, https://doi.org/10.5194/acp-25-4269-2025, 2025.

Lamquin, N., Stubenrauch, C., Gierens, K., Burkhardt, U., and Smit, H.: A global climatology of upper-tropospheric ice supersaturation occurrence inferred from the Atmospheric Infrared Sounder calibrated by MOZAIC, Atmospheric Chemistry and Physics, 12, https://doi.org/10.5194/acp-12-381-2012, 2012.

Lee, D., Fahey, D., Skowron, A., Allen, M., Burkhardt, U., Chen, Q., Doherty, S., Freeman, S., Forster, P., Fuglestvedt, J., Gettelman, A., León, R. D., Lim, L., Lund, M., Millar, R., Owen, B., Penner, J., Pitari, G., Prather, M., Sausen, R., and Wilcox, L.: The contribution of global aviation to anthropogenic climate forcing for 2000 to 2018, Atmospheric Environment, 244, 117 834, https://doi.org/10.1016/j.atmosenv.2020.117834, 2021.

Lee, D. S., Fahey, D. W., Forster, P. M., Newton, P. J., Wit, R. C., Lim, L. L., Owen, B., and Sausen, R.: Aviation and global climate change in the 21st century, Atmospheric Environment, 43, 3520–3537, https://doi.org/10.1016/j.atmosenv.2009.04.024, 2009.

Mannstein, H., Spichtinger, P., and Gierens, K.: A note on how to avoid contrail cirrus, Transportation Research Part D: Transport and Environment, 10, 421–426, https://doi.org/10.1016/j.trd.2005.04.012, 2005.

Martin Frias, A., Shapiro, M. L., Engberg, Z., Zopp, R., Soler, M., and Stettler, M. E. J.: Feasibility of contrail avoidance in a commercial flight planning system: an operational analysis, Environmental Research: Infrastructure and Sustainability, 4, 015 013, https://doi.org/10.1088/2634-4505/ad310c, 2024.

Muhsin, M., Sunilkumar, S., Venkat Ratnam, M., Parameswaran, K., Krishna Murthy, B., and Emmanuel, M.: Effect of convection on the thermal structure of the troposphere and lower stratosphere including the tropical tropopause layer in the South Asian monsoon region, Journal of Atmospheric and Solar-Terrestrial Physics, 169, 52–65, https://doi.org/10.1016/j.jastp.2018.01.016, 2018.

National Oceanic and Atmospheric Administration: Inter-Tropical Convergence Zone, https://www.noaa.gov/jetstream/tropical/convergence-zone, last access: 2025-11-24, 2023.

Neis, P., Smit, H. G. J., Rohs, S., Bundke, U., Krämer, M., Spelten, N., Ebert, V., Buchholz, B., Thomas, K., and Petzold, A.: Quality assessment of MOZAIC and IAGOS capacitive hygrometers: insights from airborne field studies, Tellus B: Chemical and Physical Meteorology, 67, https://doi.org/10.3402/tellusb.v67.28320, 2015.

Petzold, A., Thouret, V., Gerbig, C., Zahn, A., Brenninkmeijer, C. A. M., Gallagher, M., Hermann, M., Pontaud, M., Ziereis, H., Boulanger, D., Marshall, J., Nédélec, P., and Smit, H. G. J.: Global-scale atmosphere monitoring by in-service aircraft – current achievements and future prospects of the European Research Infrastructure IAGOS, Tellus B: Chemical and Physical Meteorology, 67, 28 452, https://doi.org/10.3402/tellusb.v67.28452, 2015.

Petzold, A., Krämer, M., Neis, P., Rold, C., Rohs, S., Berkes, F., Smit, H. G. J., Gallagher, M., Beswick, K., Lloyd, G., Baumgardner, D., Spichtinger, P., Nédélec, P., Ebert, V., Buchholz, B., Riese, M., and Wahner, A.: Upper tropospheric water vapour and its interaction with cirrus clouds as seen from IAGOS long-term routine in situ observations, Faraday Discussios, 200, https://doi.org/10.1039/C7FD00006E, 2017.

Petzold, A., Neis, P., Rütimann, M., Rohs, S., and Berkes, F.: Ice-Supersaturated Air Masses in the Northern Mid-Latitudes from Regular In-Situ Observations by Passenger Aircraft: Vertical Distribution, Seasonality and Tropospheric Fingerprint, Atmospheric Chemistry and Physics, 20, https://doi.org/10.5194/acp-20-8157-2020, 2020.

pycontrails: Specific humidity interpolation, https://py.contrails.org/notebooks/specific-humidity-interpolation.html, last access: 2025-04-30, 2025.

Rädel, G. and Shine, K.: Validating ECMWF forecasts for the occurrence of ice supersaturation using visual observations of persistent contrails and radiosonde measurements over England, Quarterly Journal of the Royal Meteorological Society, 136, https://doi.org/10.1002/qj.670, 2010.

Reutter, P., Neis, P., Rohs, S., and Sauvage, B.: Ice supersaturated regions: properties and validation of ERA-Interim reanalysis with IAGOS in situ water vapour measurements, Atmospheric Chemistry and Physics, 20, https://doi.org/10.5194/acp-20-787-2020, 2020.

Sanogo, S., Boucher, O., Bellouin, N., Borella, A., Wolf, K., and Rohs, S.: Variability in the properties of the distribution of the relative humidity with respect to ice: implications for contrail formation, Atmospheric Chemistry and Physics, 24, 5495–5511, https://doi.org/10.5194/acp-24-5495-2024, 2024.

Sausen, R., Hofer, S., Gierens, K., Bugliaro, L., Ehrmanntraut, R., Sitova, I., Walczak, K., Burridge-Diesing, A., Bowman, M., and Miller, N.: Can we successfully avoid persistent contrails by small altitude adjustments of flights in the real world?, Meteorologische Zeitschrift, 33, 83–98, https://doi.org/10.1127/metz/2023/1157, 2024.

Schneider, T., Bischoff, T., and Haug, G. H.: Migrations and dynamics of the intertropical convergence zone, Nature, 513, 45–53, https://doi.org/10.1038/nature13636, 2014.

Schumann, U.: On conditions for contrail formation from aircraft exhausts, Meteorologische Zeitschrift, 5, 4–23, https://doi.org/10.1127/metz/5/1996/4, 1996.

Schumann, U., Poll, I., Teoh, R., Koelle, R., Spinielli, E., Molloy, J., Koudis, G. S., Baumann, R., Bugliaro, L., Stettler, M., and Voigt, C.: Air traffic and contrail changes over Europe during COVID-19: a model study, Atmospheric Chemistry and Physics, 21, 7429–7450, https://doi.org/10.5194/acp-21-7429-2021, 2021.

Shapiro, M., Engber, Z., Teoh, R., Stettler, M., Dean, T., and Abbott, T.: pycontrails: Python library for modeling aviation climate impacts (v0.54.8), Zenodo [code], https://doi.org/10.5281/zenodo.15170914, 2025.

Shepherd, T., Polichtchouk, I., Hogan, R., and Simmons, A.: Report on Stratosphere Task Force, https://doi.org/10.21957/0vkp0t1xx, 2018.

Sonabend-W, A., Elkin, C., Dean, T., Dudley, J., Ali, N., Blickstein, J., Brand, E., Broshears, B., Chen, S., Engberg, Z., Galyen, M., Geraedts, S., Goyal, N., Grenham, R., Hager, U., Hecker, D., Jany, M., McCloskey, K., Ng, J., Norris, B., Opel, F., Rothenberg, J., Sankar, T., Sanekommu, D., Sarna, A., Schütt, O., Shapiro, M., Soh, R., Van Arsdale, C., and Platt, J. C.: Feasibility test of per-flight contrail avoidance in commercial aviation, Communications Engineering, 3, https://doi.org/10.1038/s44172-024-00329-7, 2024.

Sperber, D. and Gierens, K.: Towards a more reliable forecast of ice supersaturation: Concept of a one-moment ice cloud scheme that avoids saturation adjustment, Atmospheric Chemistry and Physics, 23, https://doi.org/10.5194/acp-23-15609-2023, 2023.

Spichtinger, P. and Leschner, M.: Horizontal scales of ice-supersaturated regions, Tellus Series B-Chemical and Physical Meteorology, 68, https://doi.org/10.3402/tellusb.v68.29020, 2016.

Spichtinger, P., Gierens, K., Leiterer, U., and .Dier, H.: Ice supersaturation in the tropopause region over Lindenberg, Germany, Meteorologische Zeitschrift, 12, 143–156, https://doi.org/10.1127/0941-2948/2003/0012-0143, 2003a.

Spichtinger, P., Gierens, K., and Read, W.: The global distribution of ice-supersaturated regions as seen by the Microwave Limb Sounder, Quarterly Journal of the Royal Meteorological Society, 129, 3391–3410, https://doi.org/10.1256/qj.02.141, 2003b.

Straka, J. M.: Saturation adjustment, p. 78–100, Cambridge University Press, 2009.

Teoh, R., Schumann, U., and Stettler, M. E. J.: Beyond Contrail Avoidance: Efficacy of Flight Altitude Changes to Minimise Contrail Climate Forcing, Aerospace, 7, https://doi.org/10.3390/aerospace7090121, 2020.

Teoh, R., Schumann, U., Gryspeerdt, E., Shapiro, M., Molloy, J., Koudis, G., Voigt, C., and Stettler, M. E. J.: Aviation Contrail Climate Effects in the North Atlantic from 2016 to 2021, Atmospheric Chemistry and Physics, 22, https://doi.org/10.5194/acp-22-10919-2022, 2022.

Thompson, G., Scholzen, C., O'Donoghue, S., Haughton, M., Jones, R. L., Durant, A., and Farrington, C.: On the fidelity of high-resolution numerical weather forecasts of contrail-favorable conditions, Atmospheric Research, 311, 107 663, https://doi.org/10.1016/j.atmosres.2024.107663, 2024.

Thouret, V., Cammas, J.-P., Sauvage, B., Athier, G., Zbinden, R., Nédélec, P., Simon, P., and Karcher, F.: Tropopause referenced ozone climatology and inter-annual variability (1994–2003) from the MOZAIC programme, Atmospheric Chemistry and Physics, 6, 1033–1051, https://doi.org/10.5194/acp-6-1033-2006, 2006.

Tompkins, A., Gierens, K., and Rädel, G.: Ice Supersaturation in the ECMWF integrated forecast system, Quarterly Journal of the Royal Meteorological Society, 133, https://doi.org/10.1002/qj.14, 2007.

Wang, Z., Bugliaro, L., Gierens, K., Hegglin, M. I., Rohs, S., Petzold, A., Kaufmann, S., and Voigt, C.: Machine learning for improvement of upper-tropospheric relative humidity in ERA5 weather model data, Atmospheric Chemistry and Physics, 25, 2845–2861, https://doi.org/10.5194/acp-25-2845-2025, 2025.

Wilhelm, L.: Meteorological Conditions for Strongly Warming Contrails and the Statistics of Contrail's Instantaneous Radiative Forcing, Master's thesis, University of Hohenheim, 2022.

Wilhelm, L., Gierens, K., and Rohs, S.: Weather Variability Induced Uncertainty of Contrail Radiative Forcing, Aerospace, 8, https://doi.org/10.3390/aerospace8110332, 2021.

Wilhelm, L., Gierens, K., and Rohs, S.: Meteorological Conditions That Promote Persistent Contrails, Applied Sciences, 12, https://doi.org/10.3390/app12094450, 2022.

Wolf, K., Bellouin, N., and Boucher, O.: Long-term upper-troposphere climatology of potential contrail occurrence over the Paris area derived from radiosonde observations, Atmospheric Chemistry and Physics, 23, https://doi.org/10.5194/acp-23-287-2023, 2023.

Wolf, K., Bellouin, N., Boucher, O., Rohs, S., and Li, Y.: Correction of ERA5 temperature and relative humidity biases by bivariate quantile mapping for contrail formation analysis, Atmospheric Chemistry and Physics, 25, 157–181, https://doi.org/10.5194/acp-25-157-2025, 2025.

Yin, F., Grewe, V., Frömming, C., and Yamashita, H.: Impact on flight trajectory characteristics when avoiding the formation of persistent contrails for transatlantic flights, Transportation Research Part D: Transport and Environment, 65, 466–484, https://doi.org/10.1016/j.trd.2018.09.017, 2018.